# POLYMERIC MATERIALS FOR CORROSION PROTECTION IN GEOTHERMAL SYSTEMS

by

JENNIFER C. ESPARTERO

Submitted in partial fulfillment of the requirements
For the degree of Master of Science

Thesis Advisor: Dr. Rigoberto C. Advincula

Department of Macromolecular Science and Engineering

CASE WESTERN RESERVE UNIVERSITY

May 2015

CASE WESTERN RESERVE UNIVERSITY

SCHOOL OF GRADUATE STUDIES

We hereby approve the thesis/dissertation of

JENNIFER C. ESPARTERO

For the degree of Master of Science

Committee Chair

Dr. Rigoberto C. Advincula

Committee Member

Dr. David Schiraldi

Committee Member

Dr. Alexander Jamieson

Date of Defense

March 20, 2015

# TABLE OF CONTENTS

## LIST OF FIGURES

# LIST OF TABLES

# LIST OF SCHEMES

# Acknowledgement

I would like to take this opportunity to thank the significant people whom without them, this study will not be possible. But first, I would just like to thank my company, EDC, for giving me this great opportunity to turn my dream of earning a Master's degree into reality. I am always grateful each day to work in a company who shares the same vision and ethics as mine.

Next, I would like to thank Dr. Rigoberto C. Advincula for the academic supervision and guidance. I am honored to be your student and will be forever grateful for accepting and welcoming me into your group.

To the members of Advincula group, thank you all for the support and camaraderie. There was never a dull moment in the lab because of all of you. We may come from different places and of different character, but we all worked cohesively. To my mentor, the award winner, Al de Leon, saying thank you is not enough to show how I greatly appreciate all the help and teaching that you did. You were there in every step I took in this academic journey and pushed me to pick up myself every time I fall. To the Clingy Friends Society, Ms. Kat Pangilinan, Joey Mangadlao, and Sir Al, I would not achieve what I have now without all your help, support, and clinginess. You made my stay here a fun and memorable experience and I will take those clingy moments that we had wherever life takes me. Special thanks are in order as well to Ate Jenny Pyles for all the unlimited and genuine care and love. I will never forget all the help you extended to me. You all had been my home away from home.

To my ever supportive friends and family, I can't thank you all enough for all the support and prayers you have given me. I feel so lucky to have good friends and a caring family. To my parents, I dedicate this achievement for all the love you gave and the sacrifices you made to ensure a better future for me. Thank you Nanay and Pops.

To the love of my life, thank you for constantly inspiring me to become a better person each and every day. I feel so blessed having you in my life. Thank you for the enduring love and your patient heart.

Last but most importantly, to the almighty God, for all the blessings you have showered upon me, I dedicate this all to you.

# Polymeric Materials for Corrosion Protection in Geothermal Systems

## Abstract

by

JENNIFER C. ESPARTERO

Geothermal technology has gained wide attention as a new source of renewable energy but its optimum utilization is limited by accelerated corrosion. Solutions for this problem are often reactive such as regular preventive maintenance and replacement for corrosion affected components. A proactive way to solve this problem is by utilizing anti-corrosion polymers designed for geothermal brine chemistry. In this study, two different types of polymer application, an inhibitor and a coating, were evaluated for the corrosion protection of carbon steel in acidic geothermal brine. Polyvinylpyrrolidone(PVP) was used as a corrosion inhibitor while a nanocomposite composed of Polybenzoxazine, rubber, and montmorillonite (PBZ-R-MMT) was synthesized for coating application. Various characterization techniques such as Scanning Electron Microscopy (SEM), X-ray Photoelectron Spectroscopy(XPS),Fourier Transform-Infrared ( FT-IR), X-ray Diffraction(XRD), Thermal Gravimetric Anaysis(TGA), and Differential Scanning Calorimetry(DSC) were done to determine the applicability and effect of these polymers to carbon steel immersed in simulated acidic geothermal brine. The anti-corrosion properties of both the inhibitor and the coating were further tested using electrochemical techniques.

# I. BACKGROUND OF THE STUDY

## A. GEOTHERMAL ENERGY

### *1. WHAT IS GEOTHERMAL ENERGY?*

Renewable energy resources have been gaining a lot of attention due to increasing environmental awareness and initiative to decrease society's dependence on fossil fuels. An example of these resources is geothermal energy. The word geothermal (GT) comes from the Greek words *geo,* which means earth and *therme,* which means heat. Geothermal energy consists of the thermal energy stored in the Earth's crust. The most active geothermal resources are usually found along the Pacific Ring of Fire, a major plate boundaries where earthquakes and volcanoes are concentrated. Geothermal energy is mostly used for direct use and district heating, geothermal pumps, and electricity generation.

### *2. GEOTHERMAL IN THE PHILIPPINES*

The Philippines is the world's second largest producer of geothermal energy for power generation, with an installed capacity of 1.9 GW for a running capacity of about 1.8 GW, accounting for 12% of the nation's total electric power supply. The relatively high availability of the geothermal plants resulted in the delivery of about 10 TWh of generation, 17% of the nation's electricity production[1]. The Philippine geothermal industry has grown from addressing the 1970's oil crisis to paving the way for renewable energy in the country. Fig. I.1 shows the basic geothermal energy system flow which starts from extracting hot geothermal fluid from production wells going to the powerplant turbine which then produce electricity and be distributed to local electric cooperatives through the transmission lines.

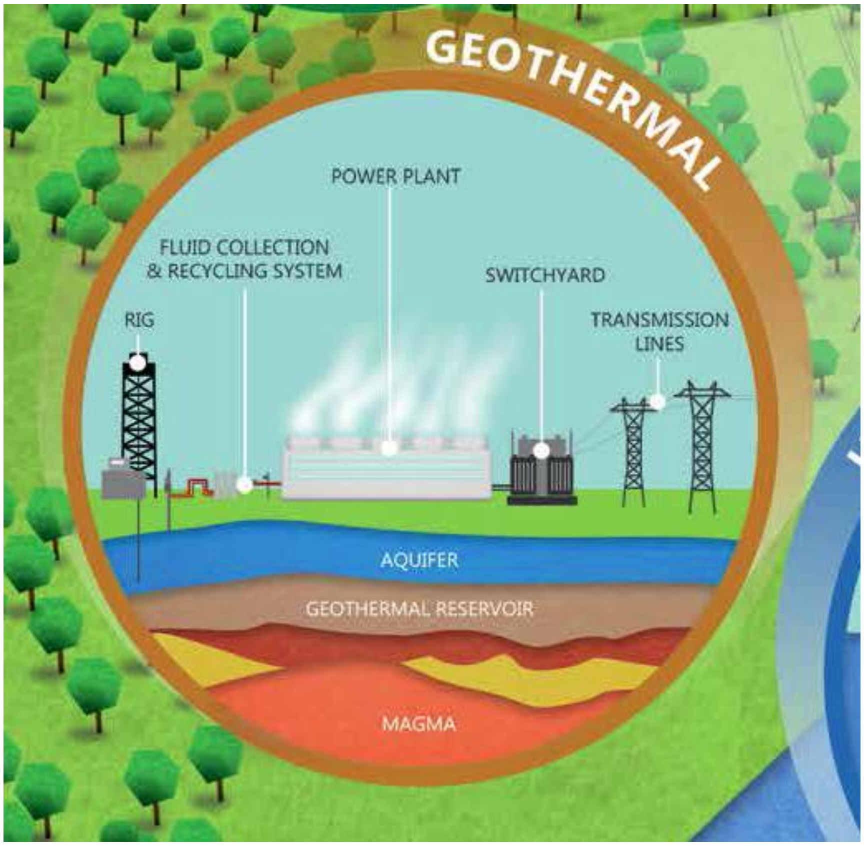

**Figure I-1. Schematic diagram of a geothermal production system.** *(adapted from EDC Annual Report 2013)*

Energy Development Corporation (EDC), the world's largest vertically integrated geothermal company, is primarily engaged in the exploration, development, operation, and optimization of geothermal steam fields and power generation. It owns 12 integrated geothermal power stations in Leyte, Bicol, Southern Negros, and North Cotabato, with an installed total capacity of 1,164 MW as shown in Fig. I.2. EDC's operations are in seven geothermal steam fields in five contract areas where the company has exclusive rights to geothermal exploration, development, and utilization through Geothermal Renewable Energy Service Contracts with the Philippine Government's Department of Energy.

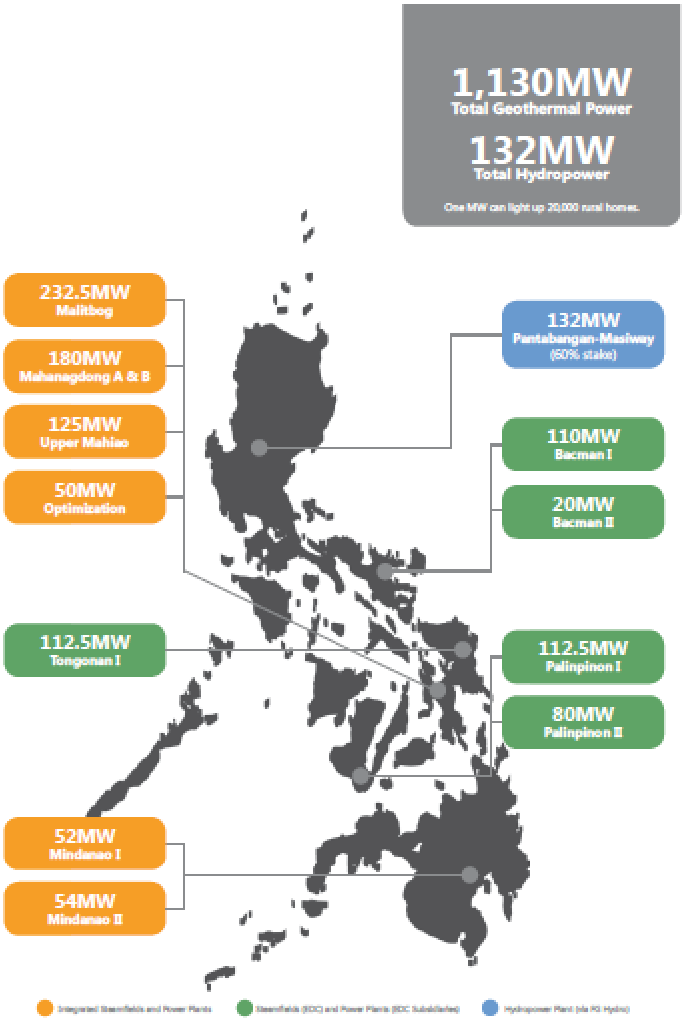

**Figure I-2 EDC's geothermal site location and corresponding installed power capacity.**
*(adapted from EDC Annual Report 2013)*

## B. PROBLEMS ENCOUNTERED IN GEOTHERMAL SETTING

Harnessing the full potential of geothermal fluids are hindered by two recurring problems, corrosion and scaling. These processes affect the operating efficiency and cause economic losses. They have a significant impact on the infrastructure starting from the wellbore of the production well to the powerplant turbine until to the pipes handling the condensates and spent brine going to the reinjection well. Below is the schematic diagram of a typical geothermal powerplant and the common problems associated with it.

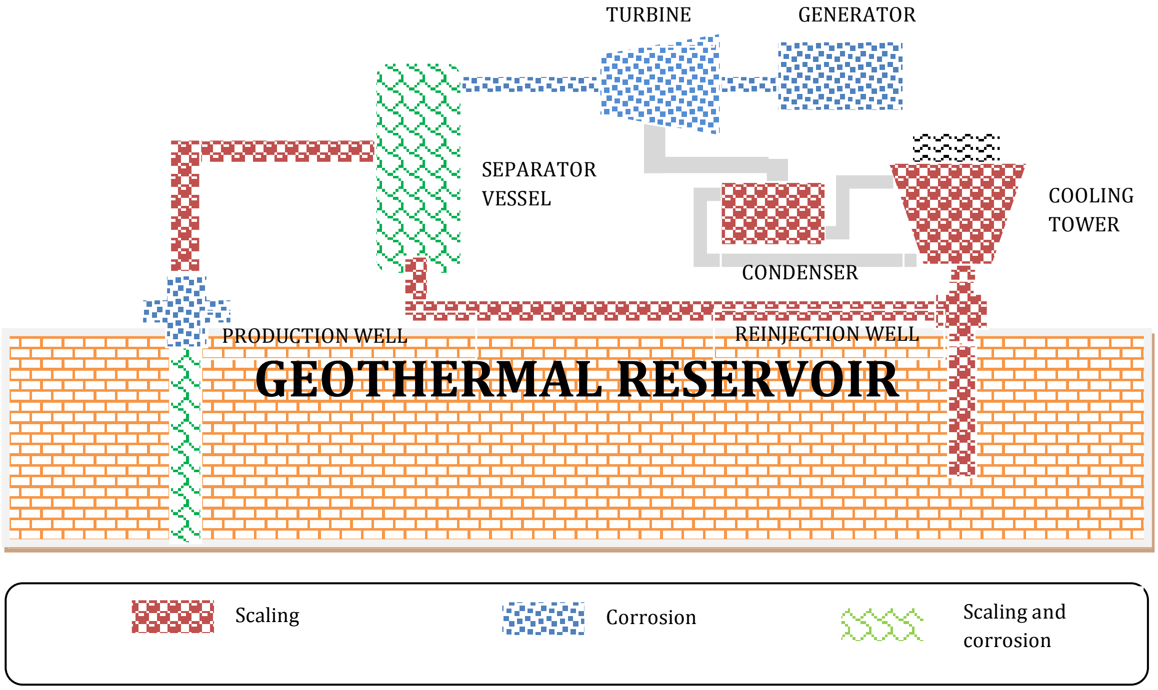

**Figure I-3 Schematic Diagram of a simple geothermal system showing problems encountered in its components.**

### 1. *SCALING*

It is innate in geothermal fluids to contain dissolved minerals. At reservoir conditions, the surrounding rocks and the fluid present are in equilibrium with each other. There is water rock interaction, thus, the minerals present in the rocks get dissolved in the surrounding brine. When this fluid get extracted for their heat, there is a change in pressure and temperature. The change of these conditions trigger the supersaturation of the dissolved minerals, causing them to be deposited along the pipelines and other components. This phenomenon is usually referred to as scaling and has an adverse effect on the power generation capability.

The common mineral deposition are calcite, silica, and sulfides. Out of these three, silica scaling is considered to be the main obstacle in high temperature hydrothermal system. Silica in geothermal brine is very soluble but after the flashing process the fluid cools off and the solubility of silica decreases, inducing the formation of silica scale[2] .

### *2. CORROSION*

Corrosion is the destructive attack of a metal by chemical or electrochemical reaction of its environment. For corrosion to initiate, it needs three elements: a cathode, an anode, and an electrolyte medium. With the absence of one factor, corrosion will not occur. In cases where corrosion has already started, retarding either the anodic and cathodic reactions can reduce the corrosion rate, thus impede further propagation. There are several methods used in corrosion control. One way is to condition the metal by either coating or alloying the metal. Another method is by modifying the corrosive environment. This is usually done by removing oxygen or by employing corrosion inhibitors. Electrochemical control can also be used to manage the rate of corrosion by using the concept of cathodic and anodic protection where current is impressed on the metal to increase the cathodic reaction rate and increase the potential, respectively. Both of which will result in preventing corrosion to persist.

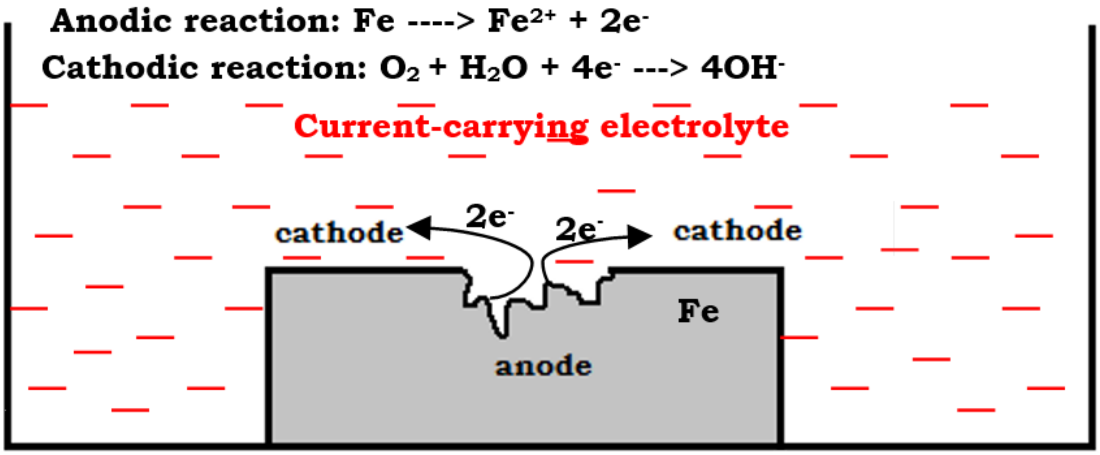

**Figure I-4 Basic corrosion process and their corresponding redox reactions .**

Due to the complexity of the corrosion reaction of the metallic components of the GT infrastructure, an in depth investigation by a specialized engineering team is required that is capable of performing detailed diagnostics of the deterioration of metals and recommendations for appropriate methods of prevention and control.

The corrosion behavior of geothermal fluid in the well and downstream pipelines, results from their chemical composition. This composition is related directly to the geological formations with which the fluids interact and percolate as they rise through the well[3]. Corrosion behavior of geothermal fluid is enhanced by its high electrical conductivity brought about by the dissolved minerals, which in turn favors the electrochemical corrosion process. Corrosion is also affected by temperature – wherein, the increase in temperature also increases the rates of chemical reactions and diffusion. Another important factor is the activity or concentration of $H^+$ ions that plays a major role in the corrosion of iron. Acidic fluids are sometimes encountered in shallow production wells, which are typically cased with carbon steels and are considered un-exploitable because of the risk of corrosion.

## C. CURRENT SOLUTIONS

### *1. MAINTENANCE SCHEDULE/MONITORING AND SCHEDULED COMPONENT REPLACEMENT*

In Southern Negros, a technical and cost assessment of silica deposition was conducted. Based from the result of their study, a cost comparison of these remedial measures with respect to the actual operating cost of the project indicates that it comprises only about 7%, and has been considered operationally tolerable[4]. Alternative options have been reviewed to improve the cost and operational efficiency of dealing with this problem. Some options, however, such as system modification to generate additional steam is restricted due to the risk of silica deposition from the supersaturated waste liquid. For this case, application of chemical inhibitors might address this constraint. The only remedial measures adopted so far are limited to mechanical de-scaling of brine lines, construction of redundant reinjection lines, and work-over and acid injection using a drilling rig, in the case of reinjection wells[5].

### 2. *USE OF INHIBITORS/PH MODIFICATION*

Organic corrosion inhibitors have been used successfully for many years to protect infrastructure carrying oil and gas. Typically, the use of the appropriate inhibitor can facilitate the use of lower grade carbon steel for pipeline construction as opposed to high grade alloys that add significant capital costs to a project[6].

For each production site, a different type of inhibition system were used depending on the significant problem that needs addressing. Table I-1 summarizes the type of inhibition system used for each specific site.

**Table I-1 Reported inhibition system applied in various EDC's geothermal sites.**

| Production field | Inhibition System employed |
|---|---|
| BGBU (Bicol) | Silica Inhibition[7-8] |
| LGBU (Leyte) | Calcite Scale Inhibition[9] |
| NIGBU(Southern Negros) | Corrosion Inhibition[10] |
| | Silica inhibition by pH modification[10] |
| MAGBU (Kidapawan) | Calcite Scale Inhibition[11] |

In Palinpinon, Southern Negros, an inhibition testing was conducted to prevent silica deposition, organic silica inhibitor and pH modification techniques are employed to delay silica polymerization until brine reaches the wellbore formation. However, organic silica inhibitors are quite expensive and an in-depth cost-benefit ratio is needed. For pH modification, it could induce corrosion problems along the line since pH reduction could increase the rate of material degradation by electrochemical corrosion process. Pilot testing are usually set-up to test the efficiency of commercial products before the actual site application[10].

The success of chemical inhibition depends mainly on the thermal stability of the inhibitor. The choice of suitable inhibitor should not be based only on the cost but on its effectiveness as well at the expected subsurface temperature and pressure of the reservoir. Field and laboratory testing is recommended prior to actual application to determine the inhibition property and thermal stability of the inhibitor[11].

## D. NEW TECHNOLOGIES TO VENTURE

Due to the harsh conditions of a geothermal condition, high performance materials are desired to lessen the frequency or even eliminate maintenance cleaning of surface components and to prolong the service life of wellbore pipes that are critically affected by erosion-corrosion phenomenon. These materials may be classified into two: 1) high performance metals that are specifically developed to a specific need 2) high performance polymers (both as a coating and an inhibitor) that could be tailored into any environment.

### *1. HIGH PERFORMANCE MATERIAL OF CONSTRUCTION*

Carbon steel is the metal of choice for both wellbore and surface pipes in the geothermal setting. It has good mechanical properties, cheap, and widely available. It's also proven to have an acceptable service life of 25 years given a corrosion rate of 0.1 mm/yr. However, under special conditions of an acid-bearing production well, the corrosion rate can be several times higher than the allowable corrosion rate. More often or not, the pipes on these type of wells corrode very quickly especially if there are also solids suspended on the steam component. This poses a safety risk of a well blow out due to degradation of the wellbore casing which served as its main structural foundation. This could warrant an earlier shut-off of the well or even cement-plug it for safety purposes. This would incur a significant financial loss. Thus, there's a need for a sturdier, more robust, and well-adapted type of material for these conditions. Various studies were conducted to determine applicability of newly developed materials of construction to high temperature, high pressure, and highly corrosive environment such as in oil and gas industries[12] . Components made of titanium alloy and stainless steel commonly are employed for dealing with these problems[13]. However, another major consideration in using these materials is the susceptibility of their corrosion-preventing passive oxide layers that develop on their outermost surface sites to react with brine-induced scales, such as silicate, silica, and calcite. This reaction leads to the formation of strong interfacial bonds between the scales and oxide layers, inducing unwanted scaling which impairs the plant component's function and efficiency. In addition, a substantial amount of time and resources are entailed in removing the formed scales. If inexpensive carbon steel components could be coated and lined with cost-effective high-hydrothermal temperature stable, anti-corrosion, oxidation, and fouling materials, this would improve the power plant's economic factors by decreasing operation and maintenance cost[14].

## *2. HIGH PERFORMANCE POLYMERS*

There are various inhibitor studies conducted at various geothermal sites in the Philippines. However, despite of the numerous studies on high performance polymer coatings which demonstrate high thermal stability, improved mechanical properties, good chemical resistance, and special attributes such as superhydrophobic and self-healing capabilities, there is no reported study on the effective use of anti-corrosion coatings in any of the geothermal sites of EDC. The use of polymer coatings, however, is limited due to their visco-elastic nature and inability to withstand high temperatures. Modern coating technology is focused to the need of developing high performance polymeric materials possessing superior mechanical, thermal, and anticorrosive characteristics to overcome the adverse environmental conditions. The fusion of organic and inorganic functionalities into a single polymer offers a unique combination of distinctive properties of both constituents such as good processability, improved toughness, flexibility, chemical resistance and some other properties like weatherability, UV resistance and thermo-oxidative stability. These hybrid polymers are already available in the market but haven't been tested in EDC's geothermal sites due to their high cost and difficulty of coating of components that are already installed. Polymer hybrids are discussed below for this possible application.

### a) High performance coatings

Polymer nanocomposites consist of nanoparticles or nanofillers dispersed in a polymer matrix. Various process for preparation of polymer-based nanoparticle nanocomposites have been reported, leading to improvement in mechanical, thermal and electrical properties. When designing nanocomposites, it is important to remember that it is difficult to increase all of the desired properties at the same time so one must focus on which type of property needs the most improvement. Polymer/clay nanocomposite has been attracting a lot of interest due to the improved material properties at optimum clay loading. The improvement of mechanical properties and corrosion performance, and increase in thermal stability is dependent on the intercalation of organoclay with the polymer matrix[15-19].

Conducting polymers (CPs) such as polyaniline (PANI), polypyrrole (PPy), and polythiophene (PTh) are used for the corrosion protection of metals and metal alloys. Several groups have reported diverse views about the corrosion protection by CPs and hence various mechanisms have been suggested to explain anticorrosion properties of CPs. These include anodic protection, controlled inhibitor release as well as barrier protection mechanisms. De leon et. al. was able to electrodeposit superhydrophobic conducting polythiophene coating to effectively protect the underlying steel substrate from corrosion attack: by first preventing water from being absorbed onto the coating, thus preventing the corrosive chemicals and corrosion products from diffusing through the coating, and second by causing an anodic shift in the corrosion potential as it galvanically couples to the metal substrate. Results showed a protection efficiency of greater than 95%. One of the advantages of the process developed in this study is that the coating is simple and easy to coat to any metallic surface[20].

### b) Inhibitors

Scaling phenomenon is a costly problem to industries that handle underground water. For the past years, various polymeric inhibitors were studied and developed to control and inhibit unwanted scaling in hypersaline solution like that of a geothermal brine.

For the retardation of scaling of calcite, numerous inhibitors were tested and developed using maleic anhydride (MA) and styrene p-sulfonic sodium (SSS) as monomers. One study introduced a novel terpolymerscale inhibitor β-cyclodextrin(CD)–MA–SSS based on β-CD–MA and styrene p-sulfonic sodium (SSS) as monomers, water as solvent, and ammonium persulfate as initiator by the free-radical polymerization. Calcite scale was reduced up to 99.9% due to strong inhibition action[20]. Another study made use ofpalygorskite instead of cyclodextrin. It also showed very good inhibition efficiency[21]. The study was later modified by adding chitosan. A scale inhibitor copolymer modification with chitosan was prepared from maleic anhydride, styrene sulfonic sodium, acrylic amide and chitosan. The conditions of preparing scale inhibitor were optimized. The chemical structure and thermal property were investigated. Using the static experiment method, the influences of the copolymer concentration, temperature, time, $Ca^{2+}$ concentration, $HCO^{3-}$ concentration of the system on the inhibition efficiency were investigated. The experimental results showed that the polymer was excellent calcium carbonate scale inhibition and the resistance rate of calcium carbonate scale up to 95.62%. All of these inhibitors were reported to be applicable in systems of high temperature and high hardness water[22]. In addition, Acrylic acid (AA) and maleic acid (MA) polymers were also found to inhibit the precipitation of calcium carbonate and gypsum from supersaturated solutions to extents exceeding 90% at concentrations as low as 2ppm. The molecular weight (MW) was an important parameter in determining the activity of the tested inhibitors. Lower MW polymers (ca. 2000) proved to be more efficient than higher MW polymers. A similar trend was exhibited for the dispersion ability of the hematite particles. AA and MA copolymers in which functional groups were introduced (pyrrole, sulfono and amide groups) were efficient precipitation inhibitors and dispersion agents, but the efficiency depended strongly on the co-polymer architecture. Copolymers containing sulfono groups improved inhibitory activity and dispersion ability and showed higher calcium ion tolerance[23]. Addition of anionic vinylic monomers, vinyl phosphonic, vinyl sulfonic, acrylic acid, maleic acid and aconitic acid, to hyper-branched polyethyleneimines produced a series of polymers which have been investigated for their performance as scale inhibitors to prevent the deposition of calcium carbonate and barium sulfate. All the new inhibitors exhibited both carbonate and sulfate scale inhibition, the best performance being for the aconate-derived polymer on carbonate scale and the phosphonate-derived polymers on sulfate scale[24].

There are also several studies focusing in controlling silica scale formation. One study demonstrated the stabilization of mono- and disilicic acids by using a cationic polymeric chemical additive, polyethyleneimine (PEI), in supersaturated silica solutions at pH = 7. The PEI polymeric system contains an excess of amine groups (~25% primary amines, ~50% secondary amines and ~25% tertiary amines) that become protonated at circum-neutral pH, hence charging the molecules positively. PEI was found to be efficient as a silica scale inhibitor only at the low dosage of 10 ppm. Its inhibitory activity was found to drop as its concentration increased. It was hypothesized that PEI is entrapped into the colloidal silica matrix and deactivated. Thus, one way to maintain its activity was to create blends of PEI and anionic polymers. Anionic polyelectrolytes that were tested included polyacrylic acid (PAA), phosphonatedpolyacrylic acid ($PAA(PO_3H_2)_2$), carboxymethylinulin (CMI), poly(acrylamide-co-acrylic acid) (PAM-coAA), phosphonomethylated chitosan (PCH) are also studied for their silica scale inhibition efficiency[25]. It is observed that the silica inhibitory activity of PEI was improved upon its combination with anionic polyelectrolytes[26].

NALCO has also reported their newly- developed inhibitors. The silica inhibitor they used is a copolymer of acrylic acid and PEG methacrylate. The major active component of the co-polymer has a structure where the repeating unit in PEG varies between 5-10 with improved scaling protection compared to existing inhibitors-slope of the mass uptake on the crystal was found to be lower than during periods of time when the old treatment was in use. The new calcium carbonate inhibitor is Polyaminopolyethermethylenephosphonate(PAPEMP). One of the particular advantages of the PAPEMP molecule is its exceptional calcium tolerance. Calcium tolerance is a measure of a chemical compound's ability to remain soluble in the presence of calcium ions ($Ca^{2+}$) under both high pH and high temperature, such as in geothermal brines. As pH and temperature increases, calcium tolerance decreases rapidly for traditional $CaCO_3$ threshold inhibitors[27].

As for systems encountering both scaling and corrosion problems, a PVA hydrogel based inhibitor was developed for controlled release of solid corrosion and scale inhibitor. Liquid inhibitors are usually not satisfactory due to the high cost of fluid dosing system and the bad performance during the mixing process. These problems can be perfectly solved by solid corrosion and scale inhibitor which will be slowly released under control. As a release controller, polyvinyl alcohol (PVA) has been widely used in medical fields. In addition, it can be easily prepared. Results of the study showed an excellent performance in terms of controlled-release and corrosion-scale inhibition[28].

### E. PROMOTING SILICA SCALE DEPOSITION AS ANTI-CORROSION FILM

Most of the studies conducted in corrosion and scaling are independent of each other. There are only very few studies conducted which show the possible relationship of scaling of silica and corrosion in the geothermal setting.

A study by Mundhenk et al. present corrosion and scaling as interrelated phenomena in an operating geothermal power plant. Though there are many corrosion studies published, these results are site-specific and only give an overview of the corrosion behaviors of various materials. And though they may help in material selection, these studies doesn't usually incorporate long term experiments and the effect of scaling on the corrosion behavior- low predictive power[29].

## *1. SILICA CHEMISTRY*

In order to determine the participation of silica in the corrosion protection, its chemistry must be well understood. Silica is naturally present in nature and can be found almost anywhere. Due to its importance in geological and industrial processes, the oligomerization and precipitation of silica is well studied. Monosilicic acid, $Si(OH)_4$, is the simplest form where at ambient temperature it begins to condense to form disilicic acid. It then continues to builds up by monomer addition forming trisilicic acid and tetrasilicic acid[30]. The general rule of silica oligomerization is to minimize the uncondensed Si(OH) bonds and form Si-O-Si bonds. And at alkaline condition of pH>8, the aggregation rate is increased.

Despite the numerous silica studies conducted, only few studies were conducted to explain the polymerization of silica in acidic system. This is due to the fact that most of the industrial processes involving the use of silica is at basic condition.

## *2. SILICA BEHAVIOR IN GEOTHERMAL SETTING*

Silica scaling in various components in a water-dominated geothermal system has adverse effects in production activities and process efficiencies. Due to the huge economic losses of this process, it is a well studied matter in the geothermal community in the hope of preventing/eliminating the deposition. Precipitation of silica is strongly dependent on the temperature and pH. Kinetics also play a role on the preferential location where scaling is most likely to occur. It is considered to be a major problem in any geothermal field because of the inability to control its deposition.

However, in other industries, silica is used as solution to corrosion-related problems. This is due to the fact that SiO2 coating known for its protection of metals against oxidation and acid corrosion even at T> 300° C. It is also known to impart superhydrophobic properties when added to coating surfaces.

### *3. UTILIZATION OF SILICA IN OTHER INDUSTRIES AS ANTI-CORROSION AGENT*

There are various studies conducted regarding the use of inorganic silica films as a superior film against corrosion. These films are usually formed using the sol-gel method, an environment-friendly technique that could replace the toxic methods of coating metals for anti-corrosion. Due to its high heat and chemical resistance, SiO2 is known to improve oxidation and acidic corrosion resistance of metals under different temperatures. One study showed that enhancement was made on the corrosion protection by mixing 10 and 50 nm silica nanoparticles by sol-gel method by delaying the diffusion of corrosive species through the film[31]. Another way to enhance silica films by sol-gel method is by doping it with different kinds of corrosion inhibitors. The structure of the silica film plays a vital role on the effectiveness of decreasing the corrosion rate. Thus, it is important to take into consideration the distribution of the pores as well as the stability of the film when exposed to a corrosive media.

Another study conducted was an electro-less process for the deposition of dense and stable silica films which improved the corrosion resistance. The formation of dense film is due to the decomposition of reducing agent (sodium borohydride) which consumes the water at the metal-electrolyte interface[32]. In order to ensure uniform deposition, the concentration of monomeric species, the rate of dehydration at the metal-electrolyte interface, temperature, and pH must be optimized.

Silica has a well-characterized surface and can be modified to a wide range of functionality owing to the presence of active hydroxyl groups. The surface can be tuned to high acidic system by impregnating carboxylic functions. Hybrid materials based on organic polymers filled with silica nanoparticles present many advantages since they combine the properties of the organic phase such as flexibility, good processability and those of the inorganic phase such as mechanical strength, scratch resistance and thermal stability. Another study doped a thin acrylic coating with silica particles. Results show that the coating has very good barrier and mechanical properties. They have also determined an optimum silica nanoparticles loading of 30% where in at the value below that, they obtained greater mechanical and barrier properties. It has been reported that addition of particles and their distribution into the polymer matrix can either improve or reduce the properties. It is therefore critical to determine the optimum value[33]. This was also observed in the testing of a nanocomposite of Epoxy-poly p-phenylendiamine (EP/PpPDA) with SiO2 nanoparticles (EP/PpPDA/SiO2) as a potential corrosion inhibitors of steel in 1 M HCl solution.Enhanced corrosion protection is due to the dispersion of SiO2 nanoparticles in matrix of polymer. The protection of steel was decreased by increasing the solution temperature. Electrochemical impedance spectroscopy results showed that the corrosion inhibition of steel occurred mainly by charge transfer[34].

## *4. POSSIBLE METHODS OF PROMOTING SILICA FOR CORROSION SOLUTIONS IN GEOTHERMAL SETTING*

Though there have been no reported study on using natural silica as corrosion film in acidic geothermal environments, there are reports accounting the possible contribution of silica scale formation in reducing the corrosion rate of carbon steel in geothermal facilities.

One of the first reported observation of the formation of a protective coating is found inside the pipes carrying thermal waters used by Reykjavik Municipal District Heating Service. The thermal water formed a protective coating consisting of different amounts or iron oxide and silica. In their study they observed that the coating formed in thermal waters is much less soluble even in acid. This phenomenon was also observed on corrosion-affected pipes in Palinpinon. Rhemoroza reported that silica deposition was observed in all of the weight-loss metal coupons, even in acid-treated brine. The characteristics of the silica deposited in the acid treated brine is different from the untreated brine in that the latter deposits are hard, adherent and brittle whereas in the former the silica deposits are soft and can easily be removed[35].

Speller made an observation that silica-bearing waters were less corrosive than those in which the silica content was low. For almost a century ago, the addition of sodium silicate has been used as protection against corrosion in water systems. This was first proposed by Thresh(1922) where he noted that corrosion of ferrous materials were reduced upon addition of sodium silicate. The process was further developed by Speller(1925), Texter (1923), and Russel (1926) where they were able to show that addition of sodium silicate to hot water was able to form self-healing protective coatings[36].

This was also observed by the studies conducted by Lehrman and Shuldener. They showed that the coatings formed on the metal mainly consist of metal oxide and silica. The formation of the film in dilute silica solution is dependent on the presence of small quantities of corrosion products on the metal surface. They also examined the films produced over time and microscopically showed that there are two layers present with silica as the major component of the top layer exposed to the aqueous medium. When the hydrous metallic oxide film has been covered with a silica layer, further deposition is stopped, which accounts for the observed fact that prolonged exposure to silicate solutions does not build up thick films and that the thin films when mechanically damaged are self-healing. The attraction of positively charged corrosion-products and negatively charged silica is therefore assumed to be part of the mechanism[37].

## F. OBJECTIVE

The objective of this study is to be able to demonstrate the application of polymeric materials as better alternative solution to the challenging corrosion problems encountered in geothermal industries. The study comprises of two parts. First is the investigation of the corrosion inhibition of Polyvinylpyrrolidone(PVP) on carbon steel immersed in acidic geothermal brine by promoting silica layer formation. The objectives of this part of the study are as follow:

1. Determine the inhibitor concentration at which the PVP is soluble in the acidic geothermal fluid
2. Measure the corrosion rate of carbon steel in acidic geothermal fluid in the presence of varying molecular weight of polymeric inhibitor.
3. Determine the real time change in the corrosion rate of carbon steel in acidic geothermal fluid in the presence of varying concentration of the polymeric inhibitor.
4. Determine the effect of temperature on the corrosion rate of carbon steel in acidic geothermal fluid in the presence of varying concentration of the polymeric inhibitor.
5. Propose a possible mechanism of corrosion inhibition action of the polymeric inhibitor

The second part of this study is the synthesis and evaluation of a polymer/clay nanocomposite as a suitable anti-corrosion coating for geothermal system components that are heavily affected by corrosion with the following specific objectives:

1. Exfoliate MMT by cationic exchange between sodium and an organic surfactant
2. Prepare a toughened nanocomposite coating system composed of PBZ, rubber, and oMMT.
3. Investigate the applicability of the nanocomposite coating for geothermal applications.
4. Determine the corrosion protection efficiency of the nanocomposite coating with varying oMMT loading on carbon steel immersed in acidic geothermal fluid.
5. Propose a possible mechanism on the enhancement of the protection efficiency of toughened PBZ coating after adding oMMT

## G. SCOPE AND LIMITATIONS

In order to ensure the same chemistry of the immersion fluid, the geothermal brine used in the studies conducted was simulated based on the brine chemistry of an acidic geothermal well. The immersion studies done were only static which does not incorporate the effect of fluid dynamics. Due to the possibility that oxygen may intrude to any geothermal process, no method was done to remove the dissolve oxygen present on the simulated brine used and that dissolved oxygen at temperatures below 100° C is low.

# II. INVESTIGATION OF POLYVINYLPYRROLIDONE (PVP) AS A SUITABLE INHIBITOR IN PROTECTING CARBON STEEL FROM THE AGGRESSIVE CORROSION OF ACIDIC SIMULATED GEOTHERMAL BRINE

## A. INTRODUCTION

The use of inhibitors is considered to be one of the most economical and practical corrosion technology solutions[37-39]. However, this technology is still under utilized in EDC's geothermal fields. This is mainly due to the complexity of the geothermal brine which makes it difficult to find a compatible inhibitor available in the market. A good geothermal corrosion inhibitor should be able to control the corrosion rate at the acceptable level without causing any significant change to the brine chemistry that could lead to unwanted mineral scaling. Another factor to consider is the thermal stability of the inhibitor to be used since the process temperature of a geothermal system is between 160-350°C. In addition, inhibiting agents are effective only if their solubility in the corrosive environment is optimal. Very low solubility of inhibitor leads to lack of active agent at the metal interface and consequently to weak inhibition. If the solubility is too high, the substrate will be protected, but only for a relatively short time since the inhibitor will be rapidly leached out from the coating[40]. Due to the dissolved minerals in any given geothermal brine, its ionic strength is high. This would limit the use of polymers that are not stable at high ionic medium. Instead of dissolving, they precipitate out from the solution. Because the pH of each geothermal well is different, the use of pH sensitive polymers may also not be suitable for the application. The pH range at which the inhibitor is soluble should be broad so that it has a wide scope of application and for it to be economical and practical. In addition, a good corrosion inhibitor should satisfy the following requirements: a) it should easily oxidize the metal surface to form an impervious and compact film b) it should have highly disposable sites for chemisorption to take place onto the metal surface c) the barrier film must be able to cover a large area of the metal surface d) it should be polymeric in nature or be able to polymerize on the surface of the metal e) eco-friendly, low cost, safe in handling, and readily available [41-44].

Based on the evaluation conducted, the polymer that possess the recommended properties as a suitable corrosion inhibitor in acidic geothermal system is Polyvinylpyrrolidone (PVP). PVP has kept attracting great attention in the field of colloid and interface science because it was found that various stable oxide or metal colloids could be attained with PVP addition. It is generally agreed that PVP exhibits mesomeric structures. The structures make it possible for PVP molecules to form hydrogen bond or coordination linkage with various oxides or metals (Fe, Mn, Co, Zn, and Ni)[45]. Another advantage of using PVP is it has been reported to promote deposition of silica[46]. It is widely reported that films formed by silica are good anti-corrosion coating[47-49]. Despite the abundance of silica in geothermal brine, it is not easily deposited in low pH conditions since it is present in solution as silicic acid, which is very soluble in the brine and tends to be well dissolved in solutions. If the deposition of silica could be promoted by PVP, it could act not only as a corrosion inhibitor but can also add as an additional barrier from the corrosive species present in the brine.

## B. MATERIALS AND METHODOLOGY

Polyvinylpyrrolidone(PVP) purchased from Aldrich chemicals with varying molecular weights( 10K, 40K, and 360K ) were used as received.

### *1. SUBSTRATE PREPARATION*

The carbon steel(CS) sheets were first cut into1.5 x 2.0 cm pieces and were prepared according to the ASTM G1 standard. They were then sonicated in acetone for 15-20 min, dried, and kept under vacuum prior to use.

### *2. IMMERSION STUDY*

Polished CS were immersed in 100 ml of simulated geothermal brine in a Nalgene container with cover at varying MW(10K, 40K,and 360K), varying concentrations (5 ppm, 10 ppm, and 15 ppm), varying duration (2 days, 7 days, 14 days, 30 days, and 60 days), and varying temperature (25°C and 180°C).

### *3. WEIGHT LOSS ANALYSIS*

The carbon steel specimens were weighed on an analytical laboratory scale (precision $10^{-4}$g) and completely immersed vertically in the simulated acidic geothermal brine for 2 and 4 weeks at room temperature. After immersion, the corrosion products were first removed mechanically using a paper towel and a nonmetallic bristle brush. Then, chemical cleaning was followed in an ultrasonic bath with coupons immersed in the solution specifically designed to remove the corrosion products with minimal dissolution of the base metal. For this study, an aqueous solution of 250 ml/L HCl containing 3.5g hexamethylenetatramine was used for pickling the surface of carbon steel. The coupons were weighed on the same analytical scale.

## 4. *INSTRUMENTATION*

The FT-IR spectroscopy was done with Cary 600 Series FTIR Spectrometer (Agilent Technologies) and scanned between 4000 and 400 cm−1. All spectra were recorded with nominal spectral resolution of 2 $cm^{-1}$ and 128 scans were collected and averaged for each spectrum.

Electrochemical measurements for the evaluation of anti-corrosion property were done using Autolab PGSTAT 12 Potentiostat (MetroOhm, Inc.), with platinum as the counter electrode, Ag/Ag+ in 0.5 M NaCl as the reference electrode, and the carbon steel substrates as the working electrodes. Potentiodynamic polarization scan (PPS) was performed by scanning from −0.025 to +0.025 V vs Ag/Ag+ reference electrode (0.5 M NaCl) about the open circuit potential (OCP) while electrochemical impedance spectroscopy (EIS) was performed for seven frequency decades from 10 mHz to 100 kHz with an amplitude of 10 mV with respect to the OCP.

Scanning electron microscopy (SEM) analysis was done using JEOL JSM-6510LV SEM. X-Ray Photoelectron Spectrometer (XPS) analysis was done using PHI Versaprobe 5000 Scanning (XPS).

## C. RESULTS AND DISCUSSION

### *1. SELECTION OF CONCENTRATIONS TO BE TESTED*

One requirement of a good inhibitor is its good solubility in the corrosive solution, which in this case is the acidic geothermal brine. Since there was no reported study on the use of PVP as corrosion inhibitor in geothermal industries, a simple solubility test was conducted to determine the range of inhibitor concentration to be tested. PVP solutions with concentration ranging from 10-1000 ppm were prepared for the solubility test as shown in Figure II-1. The concept of Tyndall effect was applied to determine the maximum amount of PVP where it is still soluble in the desired medium. The Tyndall effect is usually given as a definitive test to distinguish between a true solution and a colloid. It involves the scattering of a beam of light as the light passes through a medium having particles of colloidal size. Figure II-1 shows the result of the Tyndall effect to solutions of increasing concentration of PVP in the geothermal brine. Based from the test conducted, PVP has an acceptable solubility at 50 ppm. However, due to economic concerns, it is desired that the optimum concentration of inhibitors should be as low as possible to lessen the cost of the inhibition system. Reducing the concentration of inhibitor in half would translate to half the cost as well of the inhibitors to be used, earning significant savings. For this study, concentration of 5, 10, and 15 ppm PVP were chosen to be tested and evaluated.

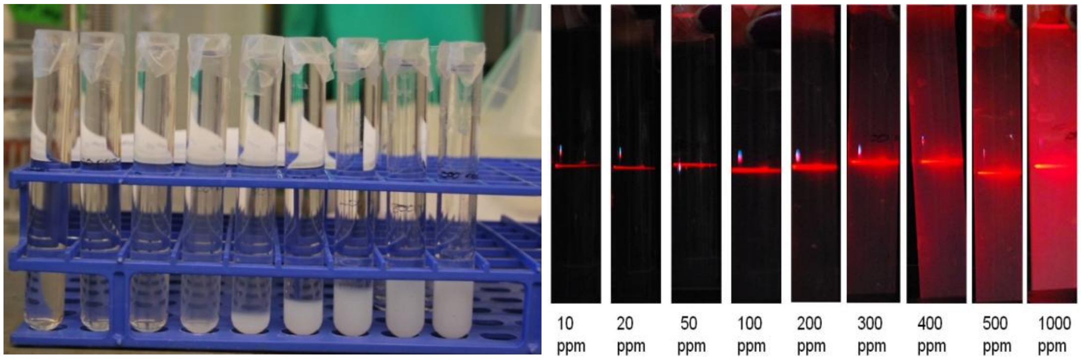

**Figure II-1Varing concentration of PVP (10, 20, 50, 100, 200, 300, 400, 500, and 1000 ppm) for solubility testing and the corresponding result of the Tyndall effect test.**

## *2. EVALUATING THE EFFECT OF MW OF PVP IN CORROSION INHIBITION*

To determine the optimum concentration of PVP, varying MW of PVP were tested using Electrochemical Impedance Spectroscopy(EIS) and Potentiodynamic Polarization Scan (PPS) tests. The inhibition efficiency of the CS immersed for one month in varying MW of PVP were determined using the Tafel analysis. This is done by varying the potential about the OCP and plotting the logarithm of the resulting current against the applied potential. Corrosion currents (Icorr) and corrosion potentials (Ecorr) were then determined by numerically fitting the resulting Tafel plots to the Butler-Volmer Equation. Icorr and Ecorr are extracted via a computer routine by specifying the cathodic and anodic branches and using non-linear least square fitting method of Levenberg/Marquardt. The corrosion rates are calculated using the equation:

$$\text{Inhibition Effficiency (IE)} = \frac{\mathrm{I}_{\mathrm{corr\ ,bare}} - \mathrm{I}_{\mathrm{corr\ ,coated}}}{\mathrm{I}_{\mathrm{corr\ ,bare}}} \times 100\%$$

Studies suggest that MW of polymeric inhibitors can have an effect on the inhibition properties due to the repulsive lateral interactions between neighboring molecules or steric effects that could hinder the adsorption of films[50]. A low (10K), mid (40K), and high (360K) MW of PVP were tested to determine the most suitable MW of PVP for an acidic geothermal system. Figure II.2 presents the corrosion rate and protection efficiencies of varying MW and concentrations of PVP immersed in acidic geothermal brine for one month.

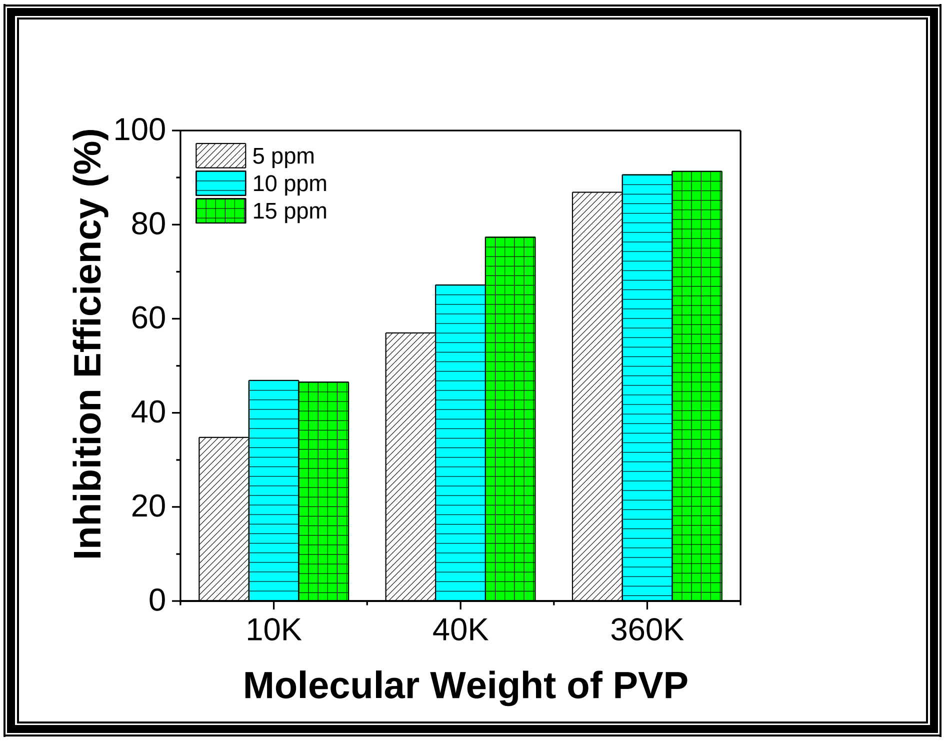

**Figure II-2 Corrosion rate and inhibition efficiencies of varying MW and concentration of PVP in brine solution.**

Results show that there is a significant increase of corrosion protection efficiency as the MW of PVP increases. This trend was also observed on the increasing concentration of PVP in acidic geothermal brine solution. Carbon steel immersed in 15 ppm of 360K PVP yields the highest corrosion protection efficiency of 91.33%. This could be attributed by the formation of silica film on the adsorbed PVP on carbon steel. It has been reported that PVP has proven to promote silica film formation on iron nanoparticles in sol-gel system .

FT-IR spectra were obtained to determine the effect of MW by comparing the amount of silica film formed on the surface by examining the stretching of Si-O bond at 1068 $cm^{-1}$. As observed on Fig. II-3, there is a direct relationship on the increasing MW to the silica found on the surface of the immersed carbon steel. Higher amount of PVP in solution would increase the quantity of PVP formed while higher MW would ensure more coverage of the film form on the metal surface. This trend was observed in the study conducted by Al Juhaiman, et.al. where the degree of protection increased with increasing PVP concentration due to the higher degree of surface coverage, which resulted from enhanced inhibitor adsorption. Steric hindrance only begins to dominate in the solution when the highest concentration of PVP is reached[51]. Since the immersion study done was in a static condition, there was no additional amount of PVP was added to the solution. This observation, however, may stand true when the study is to be conducted at flowing conditions. A separate evaluation must be conducted since increased concentration of the polymer would also lead to an increase in the viscosity which would make the transfer of polymer chains from the solution to the metal surface become more difficult.

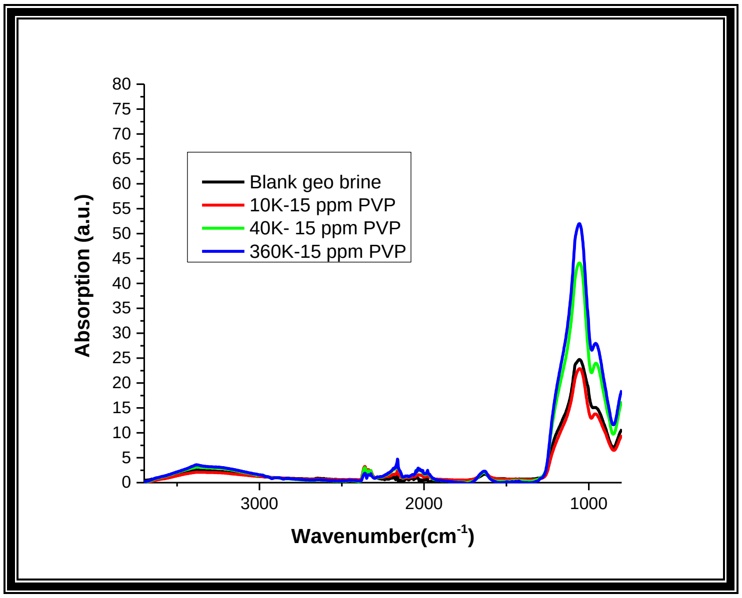

**Figure II-3 FT-IR spectra of increasing MW of PVP relating to its effect on the amount of silica formed at 1068 cm$^{-1}$**

Another important data that could be derived from the FTIR spectra is the interaction of the PVP to the surface metal. As discussed by Salehi, et.al., PVP has a carboxyl group characteristic absorption at 1660 cm$^{-1}$ and a carbon-nitrogen adsorption at 1290 cm$^{-1}$. The presence of a peak at 1293 cm$^{-1,}$ shown in Fig.II-4, of all samples immersed with PVP and none with the blank suggests that PVP is present at the CS surface. It is also apparent that as the MW of PVP increases, the intensity of the absorbance also increases which supports the result of the previous discussion.

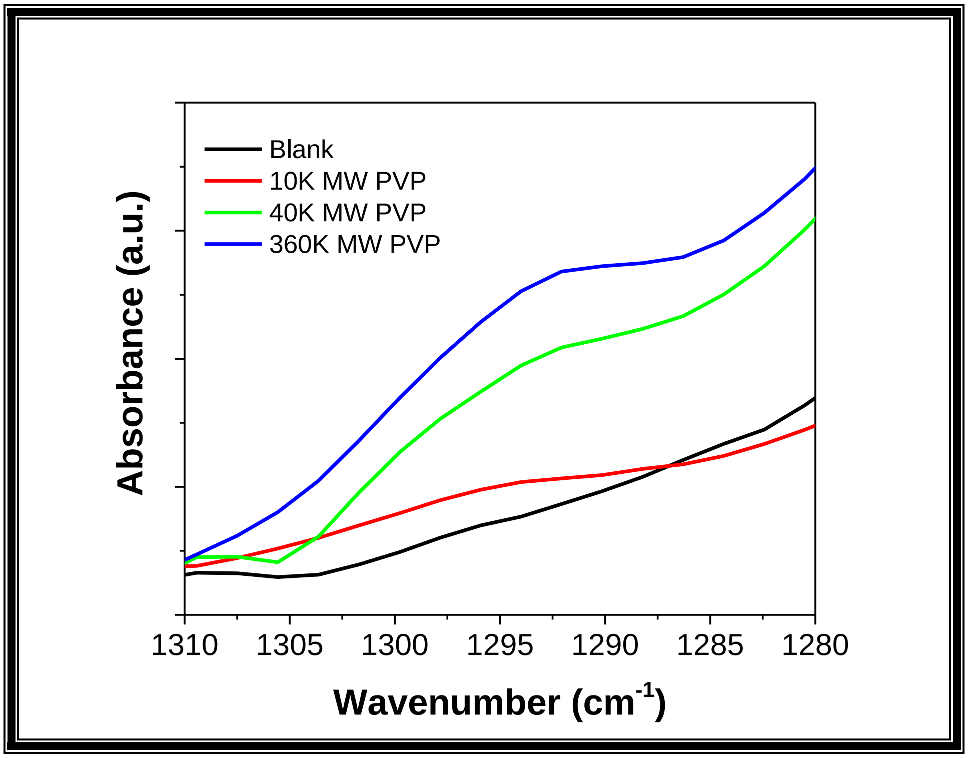

**Figure II-4 FT-IR spectra of increasing PVP relating to its effect on the carbon-nitrogen adsorption at 1290 cm-1**

It was also observed that there is a shift of the C=O absorption band of PVP from 1660 to 1630 as shown in Fig.II-5. The shift, as reported by Qiu et al, was due to the interaction of the metal surface with the PVP's carbonyl group. This could be attributed by either the reaction of the carbonyl oxygen with the metal via donation of electron pairs or the complexation of the five-membered nitrogen with the metal[52]. These findings suggest that there is a strong interaction between the PVP and the metal surface.

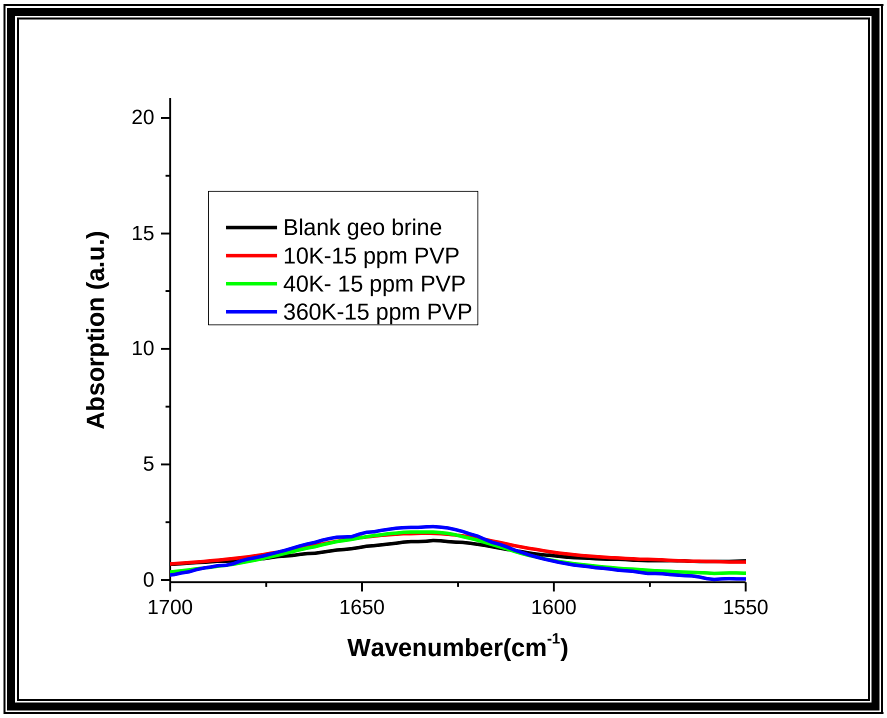

**Figure II-5 FT-IR spectra of increasing MW of PVP relating to its carboxyl group absorption at 1660 cm-1**

### *3. DETERMINING THE EFFECT OF IMMERSION TIME TO THE INHIBITION EFFICIENCY OF VARYING CONCENTRATION OF 360K PVP*

To further investigate the effect of concentration to the inhibition efficiency of PVP at its optimum MW, carbon steel samples were immersed in 5, 10,and 15 ppm PVP for 2, 7, 14, 30, and 60 days. PPS measurements were conducted to determine corrosion rate. Results were tabulated in Figure II-6.

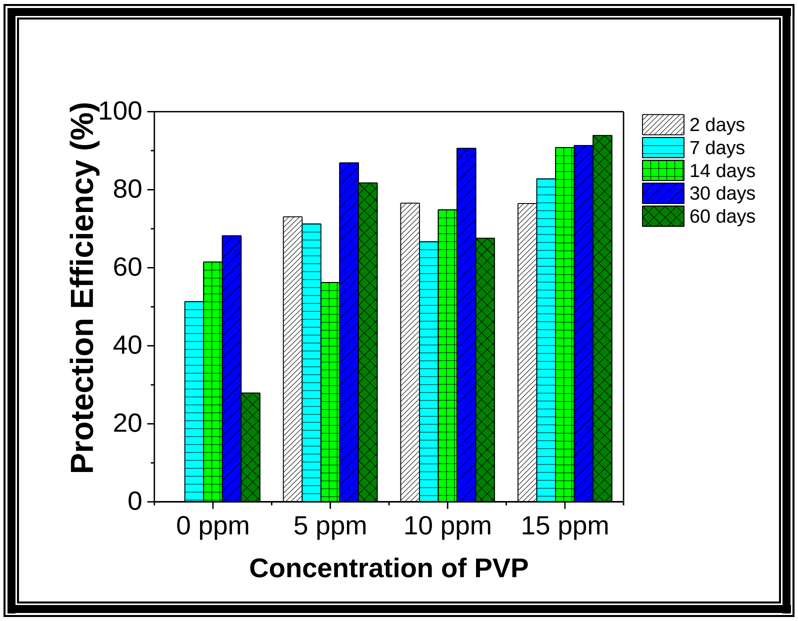

**Figure II-6 Corrosion rate of varying concentration of PVP in geothermal brine with respect to immersion time.**

In addition, weight loss analysis was also used to determine corrosion rates of different concentrations. It is the simplest, and longest-established, method of estimating corrosion losses in plant and equipment. A weighed sample of the metal or alloy under consideration is introduced into the process, and later removed after a reasonable time interval which for this study is 14 and 30 days. The coupon is then cleaned of all corrosion product and is reweighed. The weight loss is converted to a corrosion rate (CR) in mm/yr.

$$CR = \frac{m_2 - m_1}{A \cdot t \cdot \rho}$$

Where $m_1$ and $m_2$ are the weight of carbon steel after and before immersion in (mg), respectively. A is the surface area of the metal specimen (mm), t is the duration of immersion(yr) , and ρ is the density of the material (mg/mm$^3$).

**Figure II-7 Corrosion rate of CS immersed in varying concentration of PVP for 14 and 30 days**

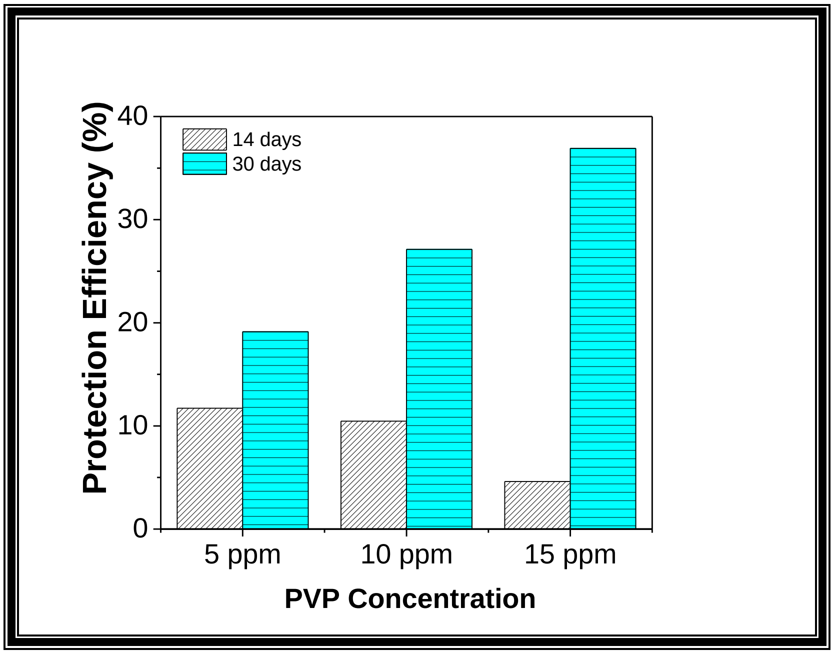

Results of the weight loss analysis in Fig. II-7 generally show a relatively lower protection efficiency as compared to the results obtained from the immersion studies. This is due to the fact that the corrosion rates of the samples have infinitesimal difference due to a short time of immersion. To be able to get a representative of the actual corrosion rate in real systems, the duration of weight loss analysis should be set longer. However, the results of the 30 day immersion show similar trend on the effect of the concentration of PVP to the protection efficiency obtained using the electrochemical analysis.

The decreasing trend of CR (and increasing inhibition efficiency) is attributed to the gradual formation of a passive film of silica. In low pH conditions, silica kinetics is slow since at this condition it favors to be dispersed in solution in its monomeric form $Si(OH)_4$ as reported by Iler. For it to be precipitated out of the solution, it needs to react to the surface. $Si(OH)_4$ can condense with any pre-existing solid surface that bears OH groups with which it can react like SiOH or any MOH surface where M is a metal that will form a silicate. In actual industrial systems, silica has never been found to precipitate on clean metal, but always a corrosion-product first for it to form. In this case, oxidation of metal and/or formation of PVP film on the metal should occur first before a silica film can be formed[53]. Another factor which may delay the formation of silica layer is that polymer units or particles formed at low pH bear no charge and aggregation begins to occur soon after polymeric particles are formed, not only because of the lack of charge on the particles, but also because the particles are extremely small and cease to grow after they reach a diameter of 2-3 nm. Since the rate of aggregation depends mainly on the number of particles per unit volume and less on their size, aggregation occurs even at low silica concentrations. Once a receptive surface is covered the condensation of $Si(OH)_4$, further deposition is silica on silica, building up a film[54].

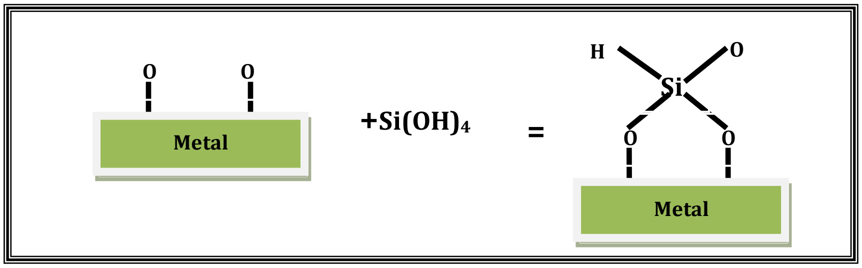

**Scheme II-1 Deposition of monomeric silica at low pH on a solid surface.**

Optical and SEM images of carbon steel immersed in different time duration support the premise of gradual build-up of silica as seen on Figures II- 8 and 9.

For samples immersed for two weeks, a thin layer is formed. However, after two weeks, it was observed that the there is a gradual build up of the film. This was supported by the IR image taken of a samples immersed in blank brine solution and with PVP shown in Fig. II-9. Compared to the sample in geothermal brine alone, the sample immersed with PVP has almost uniform deposition on the surface. For coupons immersed in solution with PVP in one month, a two-layer film was observed where the top layer is flaky, loose and porous while the layer underneath it is compact and dense. This was also observed by Remoroza et.al. on the coupons inserted in the production lines in Palinpinon which are exposed to low pH brine. it was observed that silica formation in carbon steel under acidic brine yields corrosion films that consist of two layers of silica, a thin and dense basal layer that is attached to corrosion products and an overlying porous, thicker layer of globular silica dendrites[55].

This was also observed by the studies conducted by Lehrman and Shuldener. They showed that the coatings formed on the metal mainly consist of metal oxide and silica. The formation of the film in dilute silica solution is dependent on the presence of small quantities of corrosion products on the metal surface. They also examined the films produced over time and microscopically showed that there are two layers present with silica as the major component of the top layer exposed to the aqueous medium. When the hydrous metallic oxide film has been covered with a silica layer, further deposition is stopped, which accounts for the observed fact that prolonged exposure to silicate solutions does not build up thick films and that the thin films when mechanically damaged are self-healing. The attraction of positively charged corrosion-products and negatively charged silica is therefore assumed to be part of the mechanism. The same observation was made by Demadis on his study of the inhibition and growth control of colloidal silica in water treatment industry. Pronounced silica deposition phenomena was observed on metallic surfaces that is affected by severe corrosion process[56].

| | **blank** | **5 ppm** | **10 ppm** | **15 ppm** |
|---|---|---|---|---|
| **After 1 wk** | 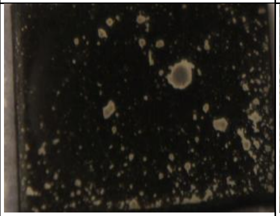 | 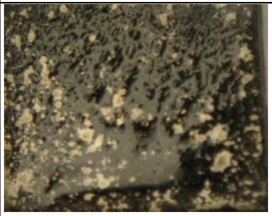 | 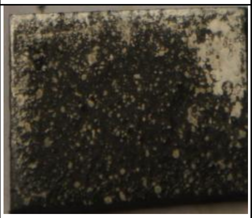 |  |
| **After 2 wks** | 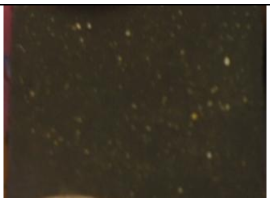 |  |  | 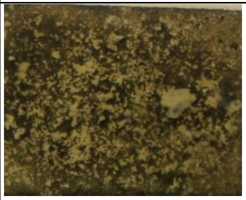 |
| **After 1 mo.** |  |  |  |  |
| **After 2 mos.** | 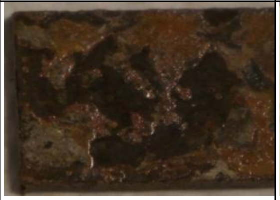 |  |  |  |

**Figure II-8 Optical images of carbon steel immersed in varying concentration of PVP in geothermal time at different immersion times**

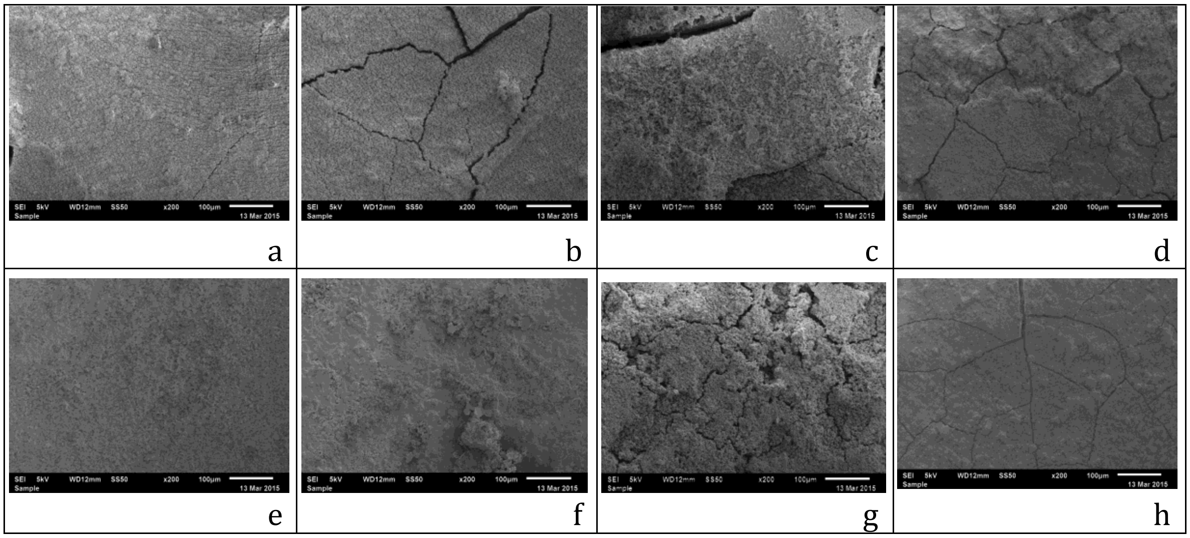

**Figure II-9 SEM images of carbon steel immersed for one month: a) top layer in blank geo brine b) top layer in 5 ppm PVP c) top layer in 10 ppm PVP d) top layer in 15 ppm PVP e) bottom layer in blank geo brine f) bottom layer in 5 ppm PVP g) bottom layer in 10 ppm PVP h) bottom layer in 15 ppm PVP**

Based on the SEM images shown in Fig.II-9, for the top layer of CS samples immersed in varying concentration of PVP, there is no apparent changes on the film formed. The top layer of all samples exhibit a compact film of silica. However, the surface of the bottom layer of these samples exhibit a significant change in terms of morphology and composition. in Fig. II.9.e shows the bottom layer of the carbon steel immersed in geo brine without PVP where metal dissolution is evident and no film was observed. Unlike in the case of carbon steel samples immersed in geo brine with PVP. A passive film is still observable and as the concentration of PVP increases, the more compact the film appears to be.

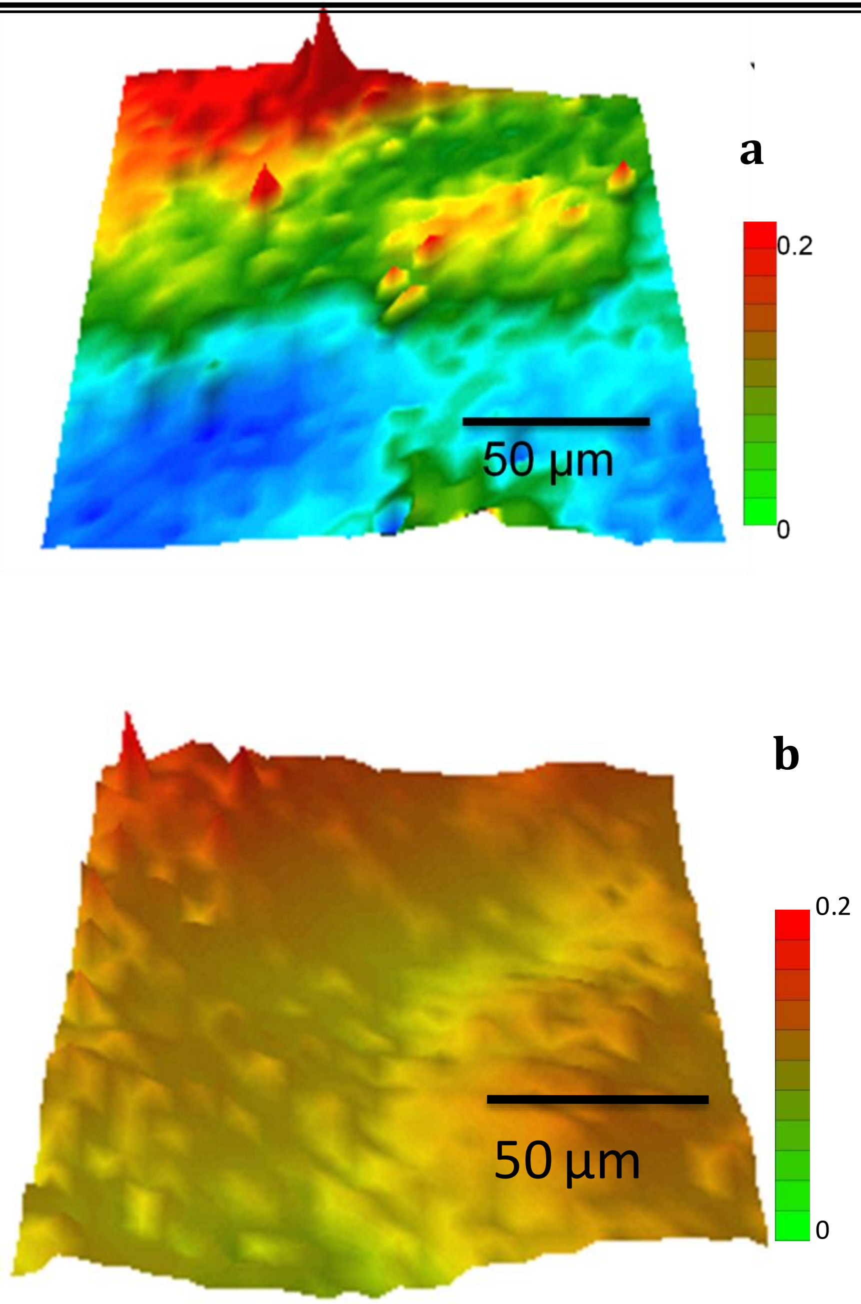

**Figure II-10 ATR IR image of carbon steel immersed in a) synthetic geothermal brine and b) with PVP focused at wavenumber 1065 (Si-O)**

Addition of PVP has a significant inhibition effect based on the EIS results gathered. EIS involves the application of a small sinusoidal perturbation to a sample under examination and the impedance modulus (z) is recorded as a function of the frequency (f). The analysis of the frequency behavior of the impedance allows the determination of the corrosion mechanism and the robustness of the passive film. To evaluate the performance of the passive film observed on the carbon steel, the impedance of the coating at the low frequency is observed. The higher the impedance at the low frequency region, the more effective the coating. As the amount of PVP increases, the impedance value of the CS immersed in it also increases (see Fig.II-11). This is mainly due to the passive layers formed as seen on both the high and low frequency region.

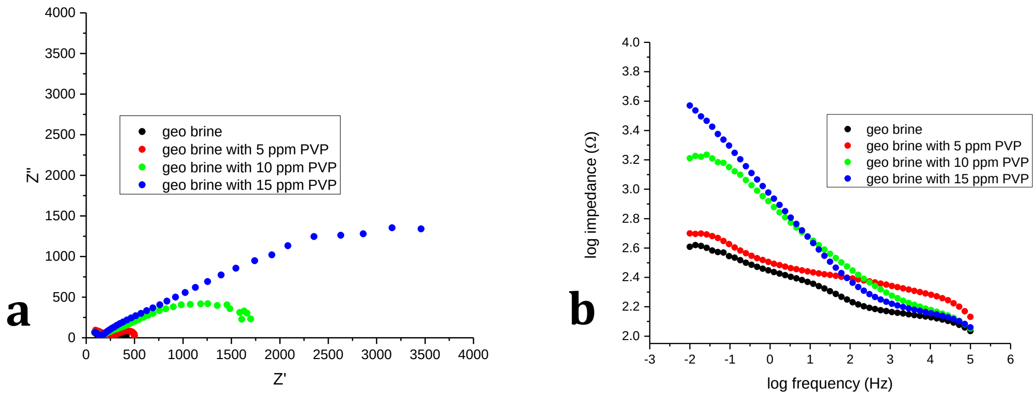

**Figure II-11 a) Nyquist plot and b) Bode plot of CS immersed in varying concentration of PVP for 1 month**

The integrity of the passive layer formed is supported by the Bode plot showing the significant difference of the passive film that was promoted by PVP as compared to the blank sample. The high inhibition efficiency of those immersed with PVP is due to the effectiveness of the passive layer formed in preventing the diffusion of corrosive species present in the acidic brine. To further investigate the formation of a 2-layer passive film, XPS analysis was conducted to determine the elemental composition of these two layers.

Results of XPS shown in Table II-1 analysis of the film form in the bottom layer of CS in geo brine alone has a significant percentage of iron which suggest that the layer is already on the metal surface. Also, the amount of silica is relatively lower compared to that found in the film of CS under geobrine with PVP. On the other hand, the iron in this sample is lower which suggest less metal oxidation. Which further supports the results shown by SEM and EIS analyses.

**Table II-1 XPS analysis of the bottom film formed in CS immersed in geobrine and in geobrine with 15 ppm PVP**

| % elemental composition | CS in geobrine | CS in geobrine with 15 ppm PVP |
|---|---|---|
| **O** | 56.9 | 60 |
| **Si** | 5.1 | 15.8 |
| **C** | 11.5 | 6.8 |
| **Fe** | 8.1 | 0.7 |
| **Cl** | 1.6 | 3 |
| **Ca** | <0.1 | <0.1 |
| **S** | <0.1 | <0.1 |
| **Mg** | 8.7 | 7.2 |
| **Na** | 8.3 | 6.7 |
| **K** | <0.1 | <0.1 |

### *4. EFFECT OF TEMPERATURE*

The inhibition property of PVP in high temperature was also evaluated by comparing the instantaneous corrosion rates of coupons immersed in varying solutions of PVP at room and actual line process temperature (160-180°C). The increase in the inhibition efficiency with the increase in temperature suggest that PVP is still thermally stable at high temperature and was able to adsorb on the metal surface. A physisorption mechanism was proposed by Umoden et.al. by considering the fact that PVP could interact with the corroding metal surface via the protonated N atom, which can be adsorbed at cathodic sites and hinder the hydrogen evolution reaction, with possible contributions from the lone pair of the electrons on the oxygen atom.  This may be facilitated by the presence of the vacant d-orbitals of iron. The adsorption of PVP creates a barrier for mass and charge transfers.

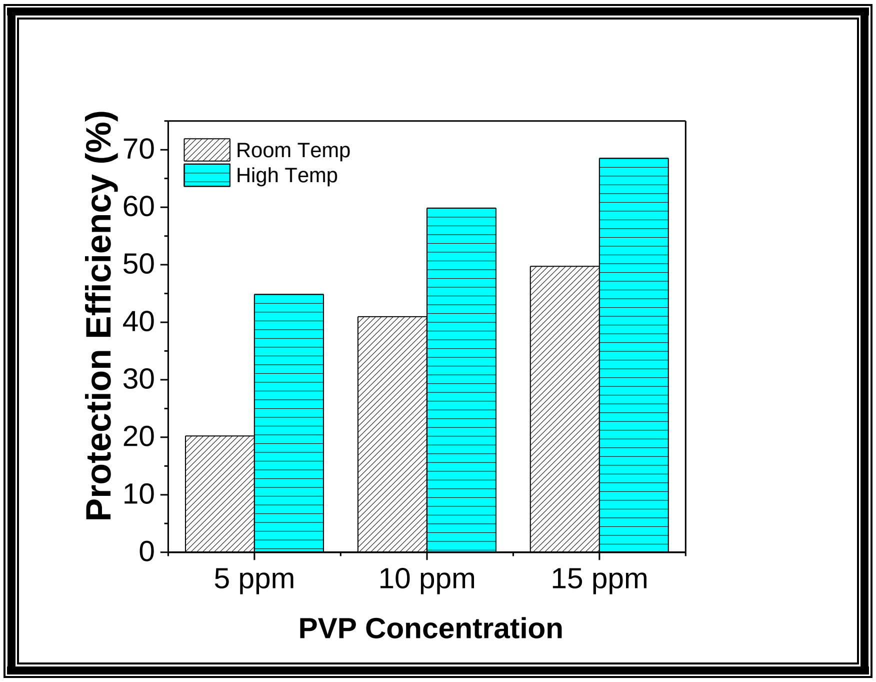

**II-12 Corrosion rates of CS immersed in varying concentration of PVP at room and line temperature (180°C)**

## 5. INHIBITION MECHANISM OF PVP

An inhibition mechanism of PVP may be deduced based on the results of the tests conducted. PVP acts as a cathodic inhibitor by forming a strong interaction with the metal, thus forming a film[46]. The polymer film formed act as seeding site for the silicic acid dispersed in the acidic geothermal to polymerize by binding to the carbonyl oxygen of PVP.

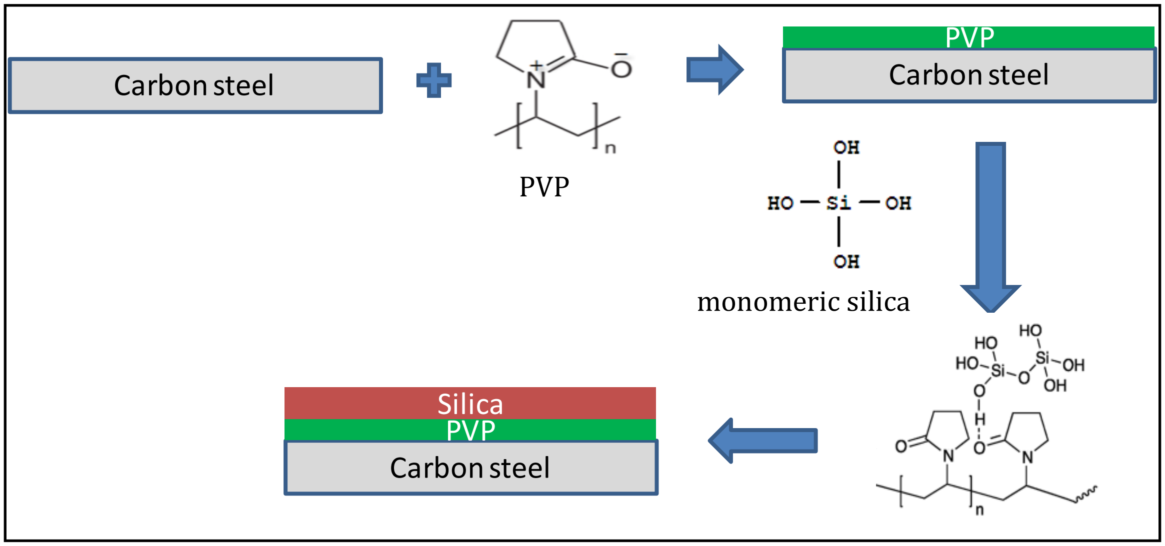

**Figure II-13 Inhibition mechnism of PVP by promoting silica.**

# III. POLYMER/CLAY NANOCOMPOSITE: A VIABLE ANTI-CORROSION COATING FOR GEOTHERMAL APPLICATIONS

## A. INTRODUCTION

One of the most common cited anticorrosion solution in geothermal industry is by pH modification by NaOH dosing which has been reported to be effective by various geothermal sites[58-59]. Though not widely used in geothermal plants, another way of retarding the effects of corrosion is by application of coatings. Due to the relatively high temperature demand of geothermal process, coatings to be applied must have good thermal stability and resistance to chemical attack. The issue of hardness and adhesion also needs to be considered in choosing the right material since geothermal fluid does not only contain corrosive agents but may contain high amounts of suspended solids. These high velocity solids will impinge on the walls of the pipe, eroding the metal. Erosion together with corrosion would have a synergistic effect on the rate of metal dissolution, making it a critical factor to consider in operating under highly erosive and corrosive environment.

Polymer modification has been attracting the attention of scientific community due to its process of combining attractive properties of different materials and fusing it into a hybrid high performance material. These properties will very much like to depend on the type of environment and its application. For this study, polybenzoxazine(PBZ) was chosen for modification on the coating application of typical acidic geothermal well. PBZ has excellent properties that fit the requirements such as near-zero shrinkage upon polymerization, low surface free energy, low water absorption, good thermal stability, and good mechanical properties[60]. Zhou et al reported that although there has been few studies conducted regarding the use of PBZ for anticorrosion, polybenzoxazines have the potential to apply as corrosion protective coating due to their unique properties such as low water absorption , low surface free energy, near-zero shrinkage , and excellent dielectric properties , which are superior to those of epoxy resins and conventional phenolics[61]. However, PBZ alone is brittle which needs to be modified to be able to expand the limits of its application[62]. Several approaches have been designed to toughen thermosetting materials and one of the most promising is the modification with rubber. It has been found that rubber modification is an effective approach to overcome the inherent brittleness of thermosets. For instance, physical blends of PBZ and rubber have improved fracture toughness without undue sacrifices to the desirable properties[63]. Hence, in this study, PBZ is toughened by blending the synthesized BZ with hydroxyl-terminated and epoxidized polybutadiene (HTBD)rubber via melt mixing. HTBD is selected as the toughening modifier. The epoxidized rubber can undergo copolymerization with the hydroxyl groups produced upon benzoxazine ring opening and thus can be chemically grafted into the matrix network[64].

To further enhance the mechanical properties of a high performance polymer material, nanofillers are usually incorporated in the polymer matrix to make up a nanocomposite. Polymer nanocomposite has been attracting the attention of the scientific community due to its ability to modify chemical and mechanical properties of a conventional polymer. Based on the study conducted by Hung et al, clay nanocomposites show enhanced physical properties even with a small amount of added clay because the nanoscale dimensions of the clay particles yield a large contact area between the polymer matrix and the filler. The structure of clays also imparts excellent barrier that provide low gas permeability and enhanced anticorrosive properties. The dispersion of clay was found to boost the thermal stability as reported by Lan et al in 1994. Enhancement on the mechanical properties was reported by Tyan et al while the molecular barrier was reported by Wang and Pinnavaia[64-67]. One critical factor is the type of nanofiller to be used. Clays are found to be one of the ideal nano reinforcement for polymers, because of its high intercalation chemistry, high aspect ratio, ease of availability and low cost based on the study of Azeez et al on epoxy clay nanocomposites[68]. It was shown that the use of montmorillonite (MMT) has enhanced the mechanical properties of the polymer at very low loading (<5 wt%)[12] . Montmorillonite is an example of smectite clay with a 2:1 structure, which allows sharing of oxygen between Al and Si. The structure of

MMT is shown in Fig.III.1. It is known to have a good high-aspect ratio, high surface area, and environment friendly. However, it is hydrophilic in its natural state which makes it difficult to be dispersed in most polymers and could easily aggregate. In order for it to be used as a nanofiller, its layered silicates should be organically modified first. This is usually done by exchanging the cations present at the silicate surfaces of MMT with long chain alkyl ammonium cation making it organophilic which will be now compatible with most polymers.

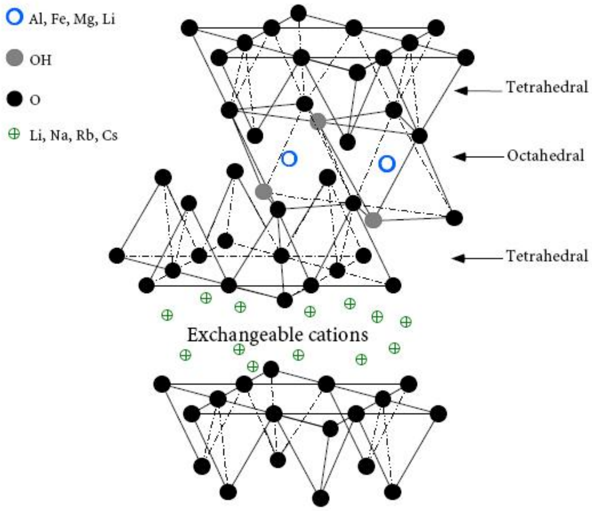

**Figure III-1 Structure of Montmorillonite[70]**

The objective of this study is to synthesize a polymer/clay nanocomposite coating that is designed for application in acidic geothermal well pipeline components and test its corrosion protection efficiency and mechanical stability under harsh geothermal conditions.

## B. METHODOLOGY

### 1. *MATERIALS*

Impact-resistant carbon steel sheets (Type A516) were obtained from McMaster Carr and was used as the substrates. The steel sheets had thickness of 0.0625 in. and composition of 0.27-0.31% C, 0.79-1.30% Mn, 0.13-0.45% Si, 0.035% P, 0.035% S, and Fe making up the remaining percentage by weight. Pro grade advanced sandpapers, used in polishing the substrates, were purchased from 3M.

99%-purity phenol and potassium permanganate (KMnO4) crystals were purchased from EMD Chemicals, Inc, while paraformaldehyde (reagent grade) and HTBD were all purchased from Sigma-Aldrich. 1,12-diaminododecane with 98% puritywas bought from TCI. Chloroform (99.8% purity) was obtained from Acros, whereas, H2SO4 (96.2% w/w), 99.9% HPLC grade tetrahydrofuran (THF), and acetone (99.7% purity) were all obtained from Fisher-Scientific.1 N NaOH solution was prepared by dissolving NaOH pellets (Fisher-Scientific, 99.4%) in Milli-Q water (18.2 MΩ cm resistivity).99.2%-purity crystalline NaCl (Fisher-Scientific) was used to prepare 0.5 M NaCl aqueous solution. All chemicals involved were used as received without further purification, unless otherwise specified.

### 2. *SUBSTRATE PREPARATION*

The carbon steel sheets were first cut into1.5 x 2.0 cm pieces, and polished with increasing grades (400, 600, and 1200) of sandpapers. They were then sonicated in acetone for 15-20 min, dried, and kept under vacuum prior to use.

### 3. *SYNTHESIS OF BENZOXAZINE MONOMER*

The difunctional linear diamine-based benzoxazine monomer was synthesized (via a modification of the solventlessmethod21), through the Mannich reaction of stoichiometric quantities (2:4:1) of phenol, paraformaldehyde, and 1,12-diaminododecane. The reactants were dry mixed and refluxed in chloroform for 16 h at a concentration of 5 mL solvent per gram of reactants. After cooling to room temperature, the crude monomer solution product was washed several times with 1 N NaOH solution and then rinsed with Milli-Q water until neutral. The washed products were dried over anhydrous sodium sulfate overnight and filtered. Chloroform was then removed by rotary evaporation, and the obtained benzoxazine monomer was refrigerated until use.

### 4. ORGANIC MODIFICATION OF MMT

Modification organically of MMT was done by using dodecyl ammonium chloride. Dodecyl ammonium chloride solution was prepared by mxing of 834 mg of concentrated HCl (12.1 N) and 1482 mg of dodecylamine in 200 mL distilled water. The mixture was stirred at 80°C until a clear solution was obtained. To this solution of dodecyl ammonium chloride, a suspension of 4000 mg of MMT in 200 mL of distilled water was added with mechanical stirring at 80°C. The stirring was continued for 5 h. The resultant white precipitate was collected by suction filtration. The precipitate was suspended in hot distilled water with mechanical stirring for 1 h to remove the adsorbed salts. This process was repeated several times until no chloride was detected in the filtrate when adding 0.1 N $AgNO_3$. The precipitate was dried in a vented oven at 100°C for 3 days and then at 110°C under vacuum for 24 h.

### 5. PREPARATION OF COATINGS

Preparation of the PBZ-R-oMMT coatings was performed by following the subsequent steps. Firstly, HTBD/BZ solution was prepared by melt mixing 20% by weight of the polybutadiene rubber with the BZ monomer under vigorous mechanical stirring at 100oC for 2 h. Secondly, HTBD/BZ solution was mixed with varying amounts of oMMT (0, 1, 3, 5,7 weight percent, with corresponding nomenclatures of PBZ-R, PBZ-R-1MMT, PBZ-R-3MMT, PBZ-R-5MMT, PBZ-R-7MMT, respectively) dissolved in THF solvent: specifically, this is done by first dispersing MMT in THF assisted by ultrasonication; HTBD/BZ solution was added afterwards, and mechanically stirred and ultrasonically mixed for 15 min each before use. In all coatings prepared, 3 g of combined weight of mmt and HTBD/BZsolution were mixed per 5 mL of the solvent THF. Thirdly, the polished substrates were dip-coated into the different coatings for uninterrupted five times with a withdraw speed of 100 mm per minute. The substrates remained in the solution for 1 minute every time. Finally, the THF solvent was evaporated by drying in an oven at 60$^{o}$C for 1 h followed by curing of the coated substrates at 200$^{o}$C for 2 h.

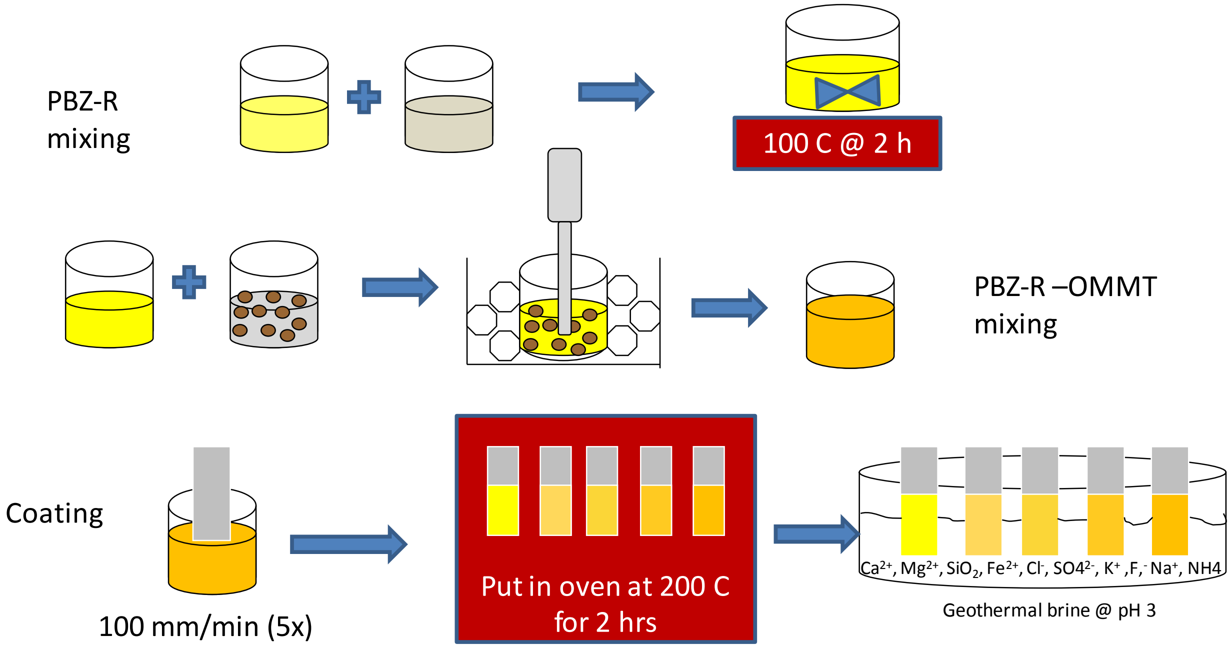

**Scheme III-1 Coating preparation of polymer/nanoclay composite**

### 6. *INSTRUMENTATION*

The FT-IR spectroscopy was done with Cary 600 Series FTIR Spectrometer (Agilent Technologies) and scanned between 4000 and 400 cm−1. All spectra were recorded with nominal spectral resolution of 2 cm−1 and 128 scans were collected and averaged for each spectrum. Thermal stability of the nanocomposites was studied using a TGA 2050 Thermogravimetric Analyzer (TA Instruments)under a continuous nitrogen or air purge (nitrogen, 70 mL/min; air, 40 mL/min). Weight loss was monitored as 5-10 mg samples of the nanocomposites were heated at a rate of 10oC/min to a maximum temperature of 700oC.

Adhesion test measurement was performed according to the ASTM standard test method D-3359 for measuring the adhesion strength by tape test. A blade handle equipped with a four-tooth 2.4-mm spacing coarse blade was used to make the cross-cut configuration through the coatings. The coating was brushed lightly with a soft brush after each cut to remove any debris, detached flakes, or ribbons of coatings from the surface. Scotch tape 51596 was placed on the cut surface and rubbed with the eraser on the end of a pencil to ensure good contact with the film and then removed rapidly after 90s. The grid areas were inspected for possible removal of the coating from the substrate and rated the adhesion strength in accordance with the scale provided by the ASTM as shown below.

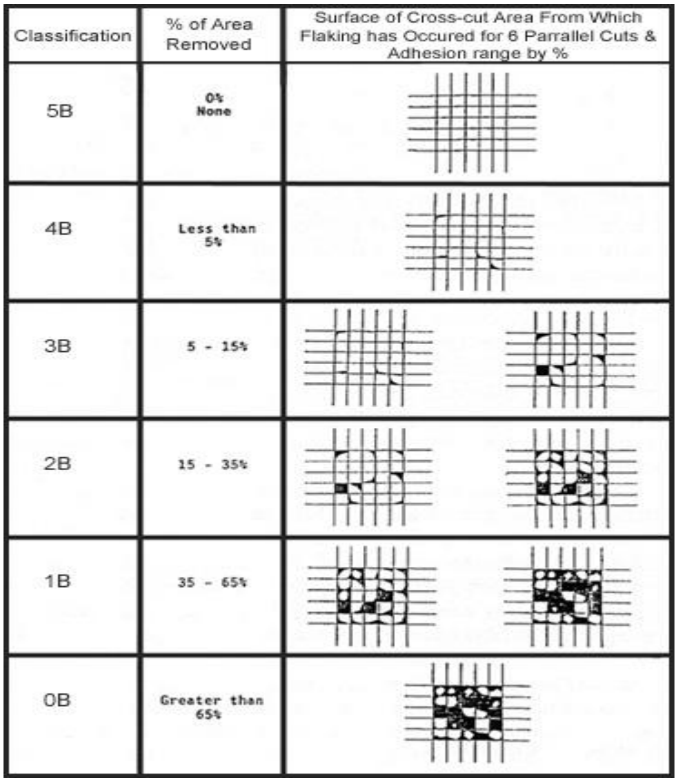

| Classification | % of Area Removed | Surface of Cross-cut Area From Which Flaking has Occured for 6 Parrallel Cuts & Adhesion range by % |
|---|---|---|
| 5B | 0%<br>None | |
| 4B | Less than 5% | |
| 3B | 5 - 15% | |
| 2B | 15 - 35% | |
| 1B | 35 - 65% | |
| 0B | Greater than 65% | |

Figure III-2 ASTM Scale for Adhesion test.

Hardness Test measurement was performed using a pencil hardness tester which meets the ASTM standard D 3363. For this test, pencils of increasing hardness values are moved over the surface in a precisely defined way until one damages the surface. Sufficient pressure must be applied to either cut or damage the coating or to crush the lead pencil point. Repeat the test as many as possible until a definite observation is made. If scratching or damage of the surface occurs, proceed with the next softer pencil grade and repeat the testing process until a pencil lead grade is found which crushes and does not damage the coating. If crushing of the hardest lead should occur, the coating is therefore extremely hard and beyond the measuring range of this test.

Electrochemical measurements for the evaluation of anti-corrosion property were done using AutolabPGSTAT 12 Potentiostat (MetroOhm, Inc.), with platinum as the counter electrode, Ag/Ag+ in 0.5 M NaClas the reference electrode, and the carbon steel substrates as the working electrodes. Potentiodynamic polarization scan (PPS) was performed by scanning from −0.025 to +0.025 V vs Ag/Ag+ reference electrode (0.5 M NaCl) about the open circuit potential (OCP) while electrochemical impedance spectroscopy (EIS) was performed for seven frequency decades from 10 mHz to 100 kHz with an amplitude of 10 mV with respect to the OCP. Lastly, scanning electron microscopy (SEM) analysis was done using JEOL JSM-6510LV SEM.

## C. RESULTS AND DISCUSSION

### *1. XRD*

One of the most critical process in ensuring optimal properties of PBZ-R-oMMT nanocomposite is the modification of the cations at the silicates interlayer spacing by cationic exchanged with long-chain alkyl ammonium cation. XRD was conducted to determine the swelling of the nanoclay by calculating the d-spacing of the natural MMT and the organically modified MMT(oMMT). Fig III.2.a shows the XRD spectra of MMT and oMMT. By using the spectra result and Bragg's law, d-spacing of MMT and oMMT are calculated to be 9.93 Å and 13.97 Å, respectively. The increase in d-spacing from the native MMT to the modified one suggests that there is expansion in the clay galleries due to the exchange of a larger molecule . This also creates a steric stabilization of the nanoclay in the polymer matrix which prevents agglomeration and lowers the surface energy. This ,in turn, will enable the oMMT to disperse well into the polymer in an organized manner creating significant improvement in the mechanical property of PBZ-R.

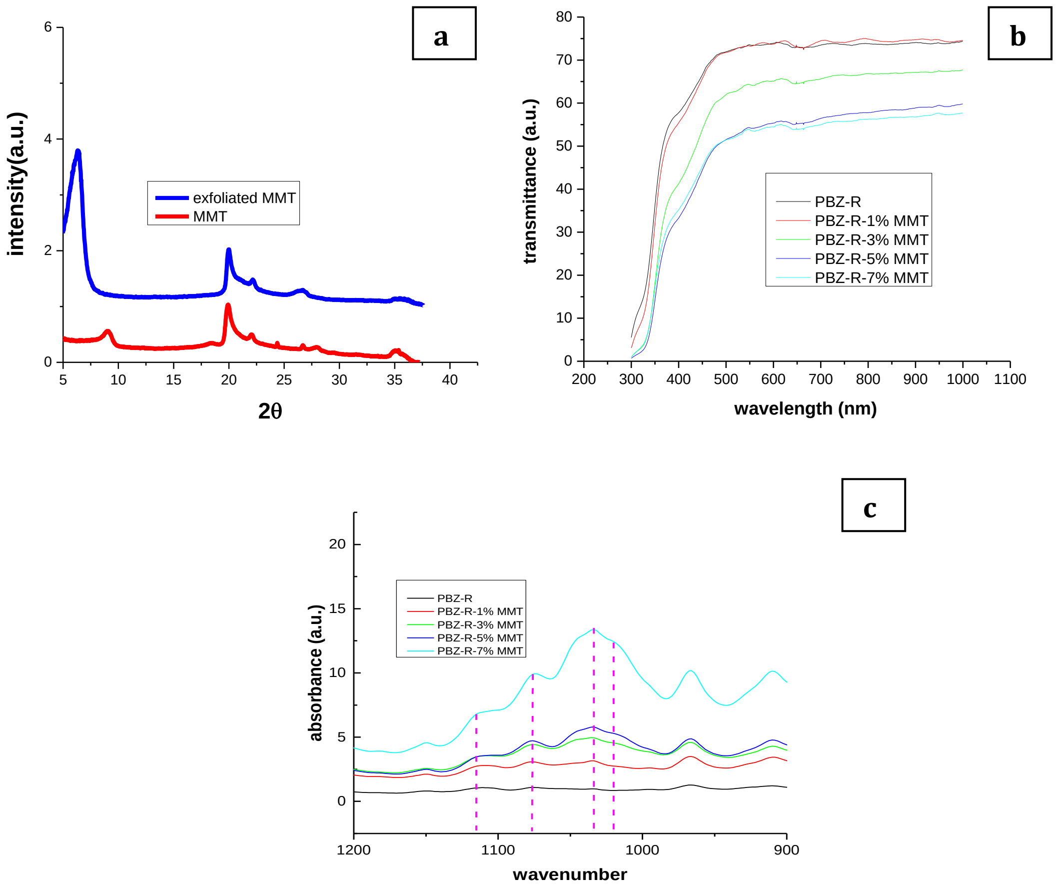

**Figure III-3 Characterization of polymer/nanoclay composite using (a) XRD (b) UV-VIS (c) FT-IR**

### *2. UV-VIS*

One of the advantages of using PBZ-R is its transparent nature in terms of aesthetic value. Clay, on the other hand, is not transparent and addition of these nanofillers may increase the opacity of the nanocomposite produced. UV-VIS was used to determine the effect of increasing MMT loading in the polymer matrix[71]. As shown in Fig.III.2b, result reveals that as the amount of oMMT increases, the transmittance of the nanocomposite decreases. Transmittance is an optical property that relates to the transparency of a material. The decrease in transmittance suggests that the nanocomposite is becoming less transparent and more opaque as the loading of oMMT is increased. Base on reported studies, there has been no significant effect on the transparency even at relatively high nanoclay loading (>20%) if the fillers are well dispersed in the polymer matrix. The result gathered, therefore, would imply that the nanofillers did not attain a fully exfoliated structure. Thus, it is recommended to lengthen the ultrasonication time to 30 minutes to achieve a fully dispersed nanoclay fillers in the polymer matrix.

### *3. FT-IR*

Studies show that improvements in the mechanical properties are directly related to the quality of the intercalation/exfoliation of the clay structure. It is important, therefore, to properly characterize the degree of layer separation. For this study, we measured the IR spectra of PBZ-R and the increasing loadings of oMMT. The spectra obtained were normalized at wavenumber ~ 2900 at the C=O stretching of PBZ and analyzed the behavior of Si-O stretching. There are 4 stretching modes of clay: I, II, III and IV with values of 1120, 1085, 1045 and 1015, respectively. The increasing stretching of these four modes are manifested in Fig. III-2c as amount of oMMT increases.

### *4. TGA AND DSC*

The enhancement of thermal stability of polymeric/clay nanocomposites is dependent on the organoclay nanofiller content and its dispersion[63]. The results of the thermogravimetric analysis (TGA) of the of PBZ-R and PBZ-R-oMMT are presented in Figure III-4a. It can be seen that PBZ-R degrades in a two-stage major weight-loss process: the first onset weight loss, which was observed at $250^{o}$C which accounts for the 20% total weight loss associated with the degradation at the Mannich bridge, an associated loss of amine-related compounds, and some weight loss related to substituted phenols in the diamine chain. The next degradation temperature starts at $430^{0}$ C which constitutes for another 60% weight loss by the degradation of phenol. This is mainly attributed by the presence of free hydroxyl groups and aliphatic-related compounds. A similar thermal behavior is found in the PBZ-R-oMMT. However, the addition of oMMT in the PBZ-R coating has resulted in a slight increase in thermal stability, as seen in the case of PBZ-R-5% oMMT, which is shown as a representative of the nanocomposite. At around 700$^{o}$C, the PBZ-R has completely degraded while the nanocomposite with oMMT has a remaining weight of about 5%. This constitute the nanoclay added in the polymer matrix which has a very high temperature degradation.

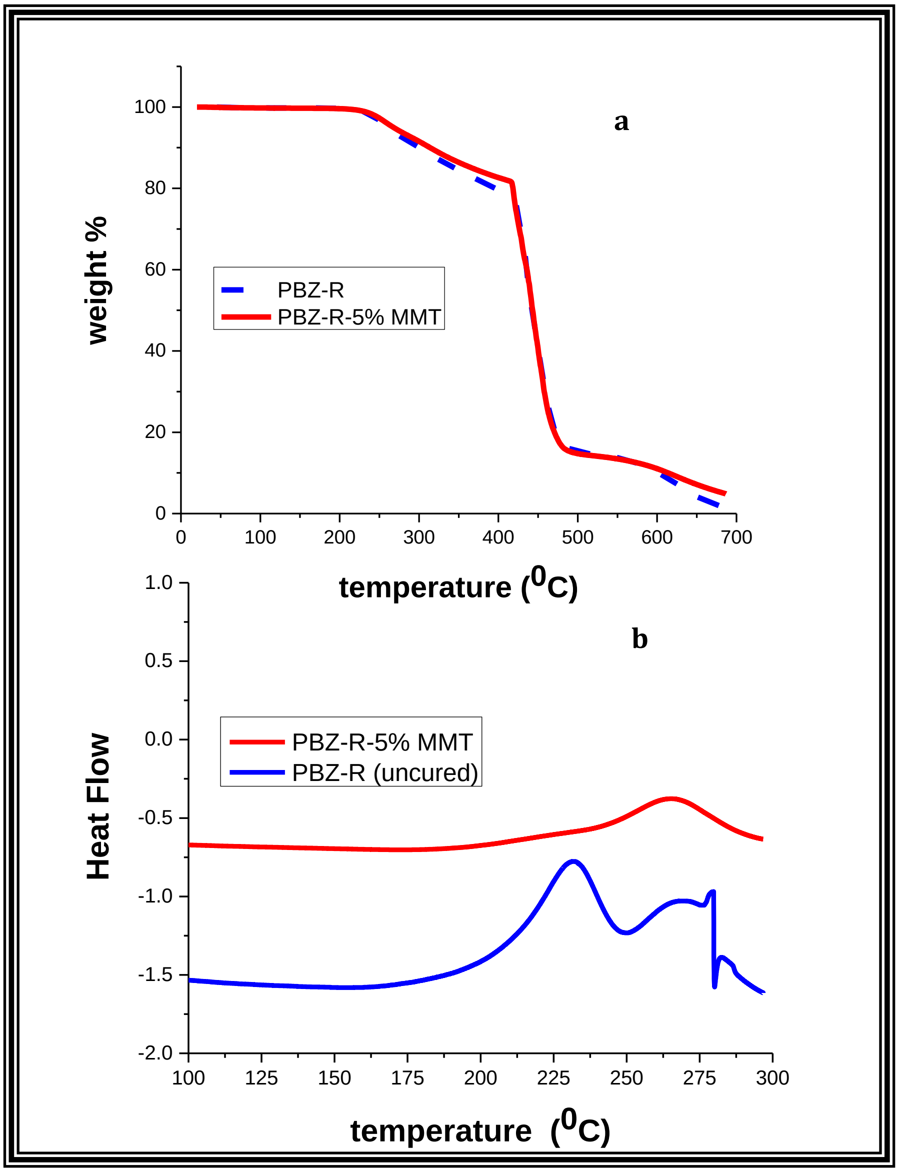

**Figure III-4 Thermogravimetric properties of PBZ-R and PBZ-R-M**

Aside from TGA, Differential Scanning Calorimetry(DSC) has been widely applied in the investigation of numerous phenomena occurring during the thermal heating of polymer/clay nanocomposites involving glass transition(Tg), melting, crsytallization and curing. DSC of PBZ-R that is uncured and the cured PBZ-R-oMMT was taken to determine the effect of nanofillers on the possible changes concerning Tg and curing temperature. Results of the DSC, as shown in Fig II-4.b, highlight the significant enhancement of the Tg of PBZ-R-oMMT as compared to the PBZ-R. Based on the DSC curve, the PBZ-R starts to phase change at $200^0$C and degrades thereafter. On the other hand, PBZ-R-oMMT is at its stable phase until around $250^0$C where it starts to undergo a phase change. This appreciable improvement is due to the confinement of intercalated polymers within the silicate galleries that prevents the segmental motions of the polymer chains[72] .

Geothermal industry operates at relatively higher temperature(~180-$200^0$C). The degradation temperatures of the fabricated nanocomposite are of the utmost importance since this would limit the application of the coating. Based on the results of TGA and DSC analysis, the nanocomposite is still in its stable form at the temperature of the intended application with no degradation or phase change.

### 5. *MECHANICAL TEST*

Many studies reported the improvement of mechanical properties of nanocomposite by addition of clay nanofillers at very moderate loadings (1-5 wt%). This improvement, however, can also be achieved by other particulate fillers like mica or talc but they need to be incorporated in the polymer matrix in a higher filler loadings (30-60%). To determine if this phenomenon also occurs in PBZ-R polymer matrix, hardness and adhesion test were conducted. Results show that even without the incorporation of clay, PBZ-R has a good mechanical property. But the addition of oMMT further improves the hardness of the nanocomposite as shown in Table III-1. The intercalation and exfoliation of MMT in the polymer matrix might have played a role in improving the tensile strength. However, addition of higher loading of oMMT could impart drawbacks due to agglomeration and difficulty of dispersion of the nanofillers. This is manifested by the decrease of hardness of the nanocomposite with 7% oMMT.

**Table III-1 Hardness and Adhesion tests results**

| | HARDNESS | ADHESION |
|---|---|---|
| PBZ-R | 8H | 5B  |
| PBZ-R-1% MMT | 9H | 5B 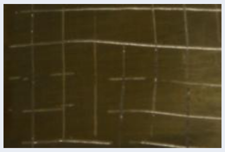 |
| PBZ-R-3%MMT | 9H | 5B 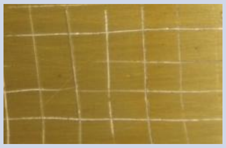 |
| PBZ-R-5% MMT | 8H | 5B 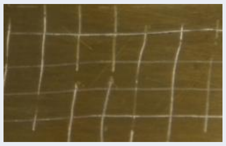 |
| PBZ-R-7% MMT | 4H | 5B  |

It is believed that clay does not actually play a role in terms of adhesion since it's the unbound hydroxyl group of PBZ-R that interacts with the metal surface[73]. However, it is also in a good note to know if the presence of clay could hinder the interaction of these free hydroxyl groups with the metal surface. Based on the results of the adhesion test, there is no significant change on the adhesion of PBZ-R alone and with increasing loadings of oMMT. The mechanical tests conducted, however, just present a preview on the improved properties since the basis of the ratings are based optically. It is suggested to do an in depth mechanical testing involving different stress/strain tests to further verify and accurately deduce the effect of addition of oMMT fillers. Its importance is mainly due to the fact that in actual geothermal systems, presence of suspended solids in the gas phase can exacerbate the corrosiveness of the brine by eroding the protective coating. A good coating, in this case, must not only be chemically-resistant and heat-resistant but has mechanical strength that could withstand the impingement of high velocity suspended particles.

### *6. ELECTROCHEMICAL TESTS*

**Table III-2 Corrosion protection efficiency of polymer/nanoclay composite coatings immersed in geothermal brine**

| | **1 day immersion** | | **7 day immersion** | |
|---|---|---|---|---|
| | **Corrosion rate (mm/yr)** | **% protection efficiency** | **Corrosion rate (mm/yr)** | **% protection efficiency** |
| **blank** | 1.03 | --- | 0.37 | 64 |
| **PBZ-R** | 0.16 | 84 | 0.02 | 98 |
| **PBZ-R-1%MMT** | 0.03 | 97 | 0.02 | 98 |
| **PBZ-R-3%MMT** | 0.06 | 94 | 0.03 | 97 |
| **PBZ-R-5%MMT** | 0.04 | 96 | 0.01 | **99** |
| **PBZ-R-7%MMT** | 0.03 | 97 | 0.01 | 99 |

To test the corrosion efficiency of the PBZ-R-oMMT nanocomposite, Electrochemical Impedance Spectroscopy(EIS) and Potentiodynamic Polarization Scan (PPS) tests were conducted. The corrosion rates of the polymer matrix PBZ-R and its varying loading were determined using the Tafel analysis after 1 day and 7 day immersion. This is done by varying the potential about the OCP and plotting the logarithm of the resulting current against the applied potential. Corrosion currents (Icorr) and corrosion potentials (Ecorr) were then determined by numerically fitting the resulting Tafel plots to the Butler-Volmer Equation. Icorr and Ecorr are extracted via a computer routine by specifying the cathodic and anodic branches and using non-linear least square fitting method of Levenberg/Marquardt. The corrosion rates are calculated using the equation:

$$\mathrm{PE} = \frac{\mathrm{I}_{\mathrm{corr\,,bare}} - \mathrm{I}_{\mathrm{corr\,,coated}}}{\mathrm{I}_{\mathrm{corr\,,bare}}} \times 100\%$$

Table III-2 summarizes the protection efficiency of samples with increased loadings of oMMT in the PBZ-R matrix. Based from the results, even without the addition of oMMT, the corrosion protection efficiency of PBZ-R is high. But with the addition of oMMT, the efficiency increases with the 7% oMMT loading the highest after one day immersion in geothermal brine. The immersion test is further extended up to 7 days to determine the prolonged exposure of the coating in geothermal brine. Clay and rubber have a tendency to swell because of the uptake of water. This swelling will cause the coating to fail since water might infiltrate the polymer matrix and reach the metal surface which, due to its aggresive chemistry as a geothermal brine, will corrode the metal. Under the film corrosion can occur even if the coating looks intact. But based on the results, the corrosion protection efficiencies increased even at longer immersion with both 5% and 7% oMMT loading being the most resistant to acid geothermal brine. The corrosion efficiency of the bare metal steel was increased because of the formation of a passive layer that retards the effect of corrosion. This is the same true for the coated samples. This passive layer could be the formation of silica film. In acidic condition, silica is in its monomeric form and does not usually precipitate out of the solution. However, given an ample enough time and the hydroxyl group of the corroded metal, monomeric silica will deposit on the corroded surface of the metal. With the protection efficiencies alone, it seems that there is no significant difference from the varying loadings of oMMT in the polymer matrix.

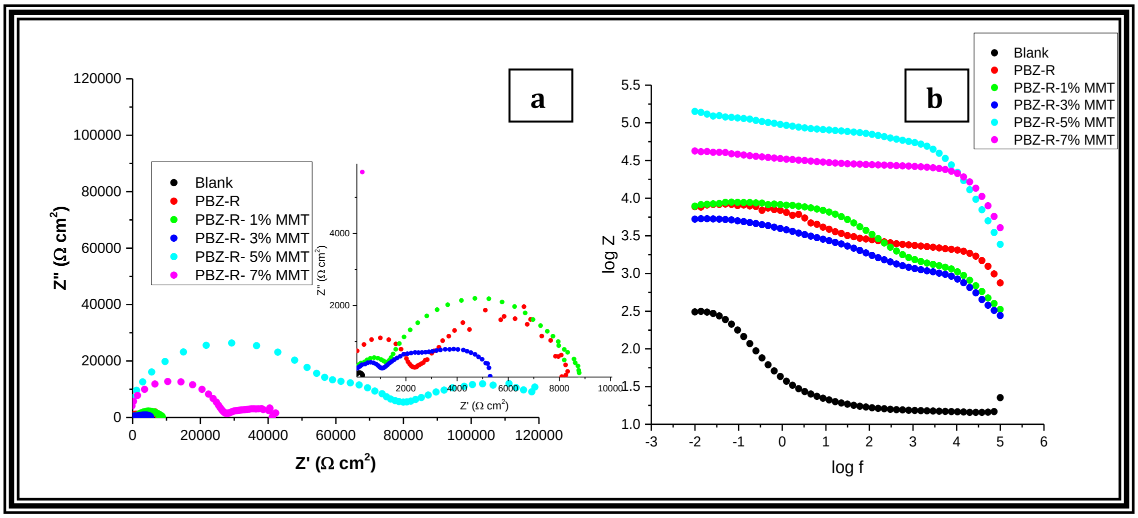

**Figure III-5 a)Nyquist plot and b) Bode plot of polymer/nanocomposite coated CS steel immersed in simulated geothermal brine for 7 days**

To further investigate this, EIS test was conducted. EIS involves the application of a small sinusoidal perturbation to a sample under examination and the impedance modulus (z) is recorded as a function of the frequency (f). The analysis of the frequency behavior of the impedance allows the determination of the corrosion mechanism and the robustness of the coating. To evaluate the performance of the coating, the impedance of the coating at the low frequency is observed. The higher the impedance at the low frequency region, the more effective the coating. The semi-circle shape of the curves shown in the Nyquist plot(Fig III-5a) suggests that the PBZ coatings are all both capacitive and resistive. The diameter of the semicircle gives the charge-transfer resistance at the electrode/electrolyte interface from which the double-layer capacitance can be calculated. As seen on the plot, the diameter of semicircle increases with increasing MMT content which implies that the charge-transfer resistance increases with the MMT loading but only up to an optimum amount after which it decreases again. For this case, the optimum loading of MMT is at 5%. The Bode and Nyquist plots shown in Fig.III-5 supports the result of the corrosion rates with the 5% oMMT having the highest impedance at the low frequency region. Despite the insignificant difference of the corrosion rate results of the EIS, the plots of Bode and Nyquist show that there is a significant difference of the impedance values of the varying amount of oMMT in the polymer nanocomposite. Also evidenced by the results is that there is an optimum loading of oMMT in the nanocomposite. At 7% oMMT loading, the corrosion protection efficiency decreases. This is due to the possible start of the coating failure as shown by the steep decline of the impedance values as compared to the 5% oMMT. This optimum value of oMMT loading is also shown by other studies on polymer/clay nanocomposite. Studies showed that addition of oMMT does enhance the mechanical properties of the polymer. However, there is an optimum amount such that adding more than that could cause agglomeration of the fillers which in turn could defeat the purpose of adding the nanofillers.

### *7. SEM*

Scanning Electron Microscopy (SEM) images were taken (Fig.III.5) to determine the morphology of the coating prior to immersion and to further verify the integrity of the coatings after 7-day immersion as shown in the figure below. Though the samples are immersed in simulated geothermal brine, a carbon steel sample in immersed in 0.5 M NaCl is also shown here to illustrate how extensive corrosion in geo brine is. There is an apparent difference on the morphology of the metal where there is obvious metal dissolution but at the same time a film deposition on the surface. This observation supports the explanation offered beforehand regarding the increase of the protection efficiency as immersion time is increased. This however should further be validated using XPS or EDX to determine if it is indeed silica that passivate the immersed samples. Before immersion, the PBZ-R and PBZ-R-5MMT coatings are almost indistinguishable having smooth surface. But after 7 day immersion, the one with 5%MMT has retained its smooth surface with no visible sign of damage or corrosion. The PBZ-R coating has shown damage and signs of corrosion. There is also signs of deposition or presence of corrosion products which should be verified by XPS or EDX studies. These observations have further verify the results of electrochemical tests conducted.

**Figure III-6 SEM images of a) bare carbon steel b) PBZ-R c) PBZ-R-5MMT before immersion in geothermal brine, d) bare steel immersed in NaCl, e)bare steel f) PBZ-R g)PBZ-R-5MMT immersed in geothermal brine for 7 days, and optical images of PBZ-R-5MMT h)before immersion i) after immersion in simulated geothermal brine for 7 days.**

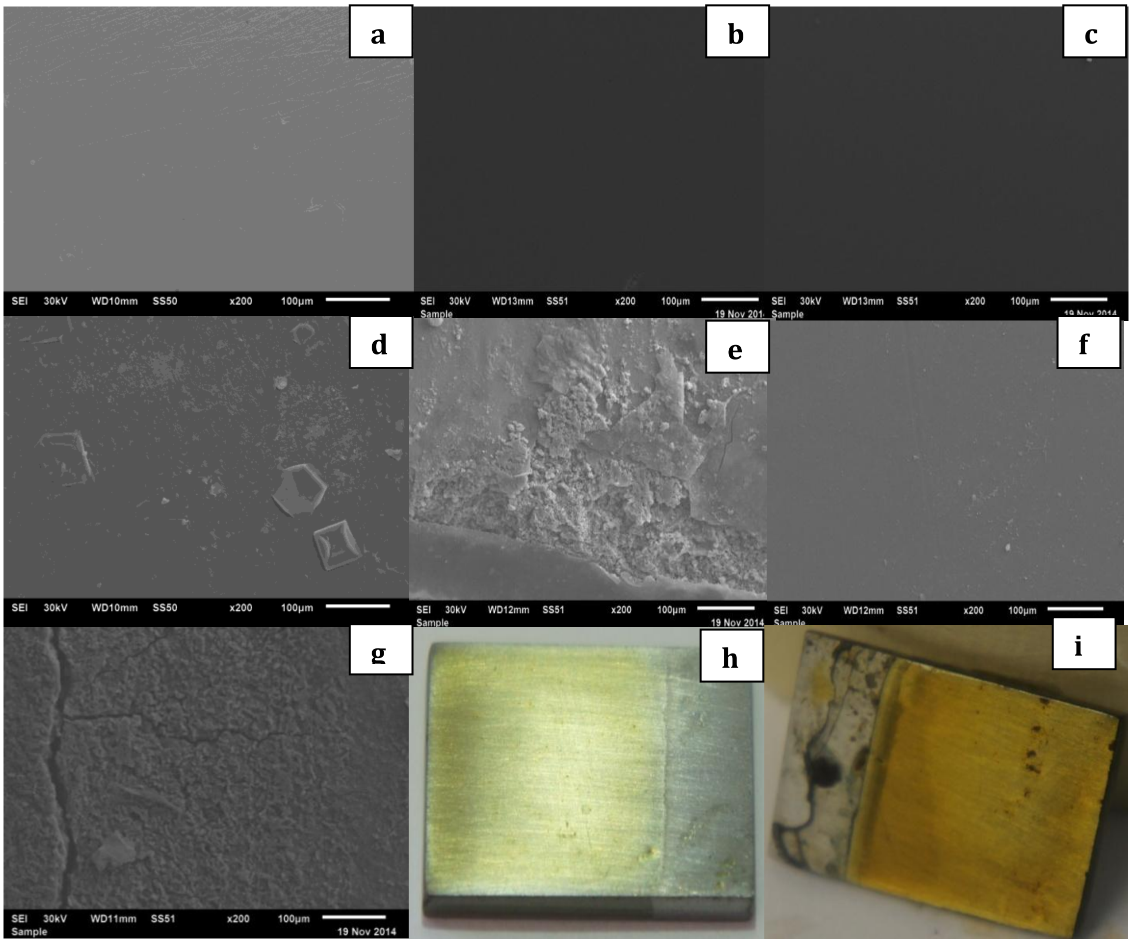

## 8. *EFFECT OF TEMPERATURE*

Since the composite coating is intended to be coated on geothermal components affected by severe corrosion, the integrity of the composite is evaluated under high temperature condition by electrochemical study. The samples were immersed separately in acidic geothermal brine in a HT/HP vessel from room temperature up to 300°C for 3 hours.

**Table III-3 Corrosion rate and protection efficiency of coated samples with varying oMMT in high temperature**

| | Corrosion Rate (mm/yr) | % Protection efficiency |
|---|---|---|
| **uncoated CS** | 1.83 | |
| **PBZ-R** | 0.13 | 93 |
| **PBZ-R-1%MMT** | 0.07 | 96 |
| **PBZ-R-3%MMT** | 0.02 | 99 |
| **PBZ-R-5%MMT** | 0.01 | 100 |
| **PBZ-R-7%MMT** | 0.02 | 99 |

Based on the protection efficiency derived from the results of PPS tests, the PBZ coatings were able to protect the carbon steel even at high temperatures as shown in Table III-3. The PBZ-R with 5% loading has a 100% protection efficiency when compared to an uncoated carbon steel. However, this value does not ensure that the coating is still intact. To evaluate further, EIS was conducted. Even at exposure at high temperature, the coating remains intact and was able to provide protection to the metal as manifested by the high impedance value of the semi-circle in low frequency region shown in Fig III.7 The occurrence of another semi-circle on the high frequency region suggests another passive layer, probably silica. The same trend was observed on the protection efficiency as that of the samples immersed at room temperature. As the loading of MMT in the composite coating increases, corrosion protection efficiency also increases with the 5% MMT as the highest. The optimum value was also observed with the decrease in efficiency of the 7% MMT. Based on the Bode plot(Fig. III-8), the nanocomposite coating with 5% oMMT loading still has the best performance compared to other loadings.

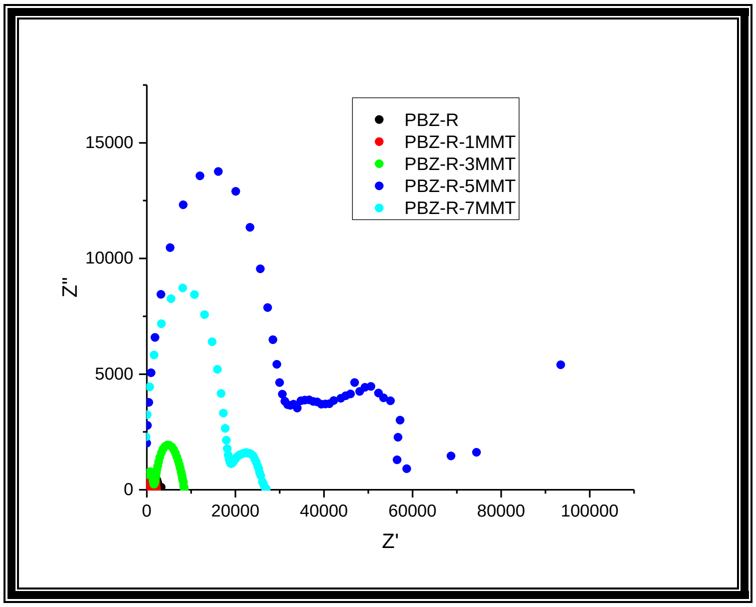

**Figure III-7 Nyquist plot of samples coated by varying amount of MMT immersed in hot acidic geothermal brine.**

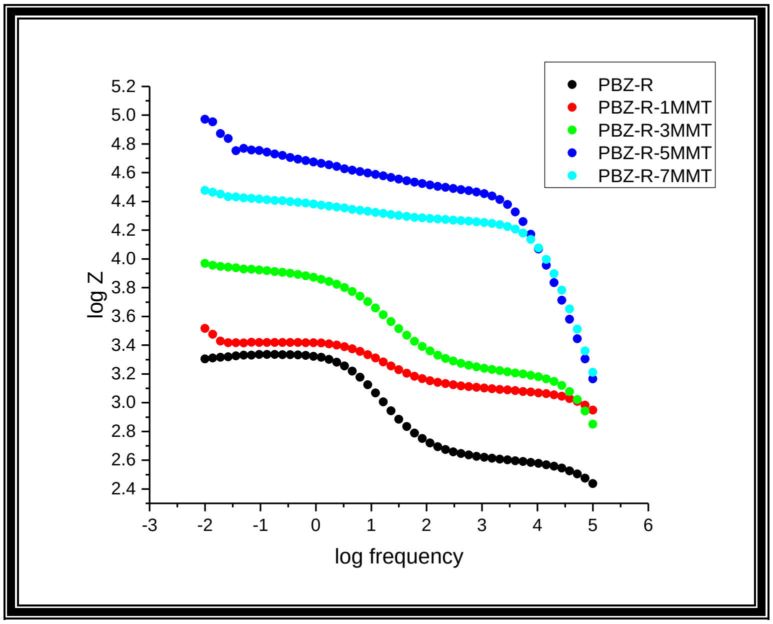

**Figure III-8 Bode plot of PBZ-R coating with varying loading of oMMT immersed in hot acidic geothermal brine.**

The mechanism of improved corrosion protection by the addition of clay nanoparticles is due to the tortous path they create which delays the diffusion of corrosive species through the coating towards the metal surface as illustrated by the figure below.

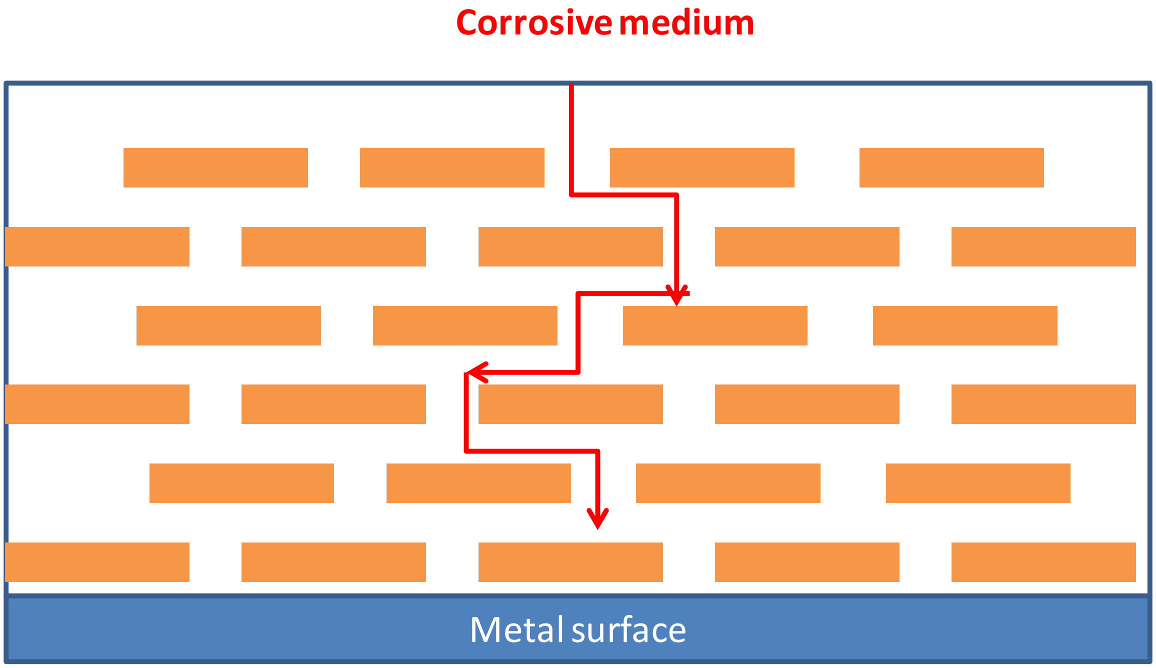

**Figure III-9 Protection mechanism of clay nanoparticles dispersed in a polymer matrix.**

# IV. CONCLUSION

Geothermal technology has gained wide attention as a new source of renewable energy that would decrease the dependence on fossil fuels and is more environment friendly. Its optimum utilization, however, is limited by massive scaling and accelerated corrosion. Solutions for these problems are often reactive such as regular preventive maintenance and replacement for scaling and corrosion affected components, respectively. A proactive way to solve these problems is by utilizing polymers designed for geothermal brine chemistry. In this study, two different types of polymer application, an inhibitor and a coating, were applied for the corrosion protection of carbon steel in acidic geothermal brine. Polyvinylpyrrolidone(PVP) was used as a corrosion inhibitor while a nanocomposite composed of Polybenzoxazine, rubber and organically modified montmorillonite (PBZ-R-oMMT) was synthesized to be used as a coating.

This study was able to determine the inhibitor concentration at which the PVP is soluble in the acidic geothermal fluid by a simple solubility technique using Tyndall effect. The corrosion rate of carbon steel in acidic geothermal fluid in the presence of varying molecular weight of polymeric inhibitor was determined and evaluated. For this study, inhibition efficiency increases as MW increases since it is only dependent on the surface area of the metal covered by the PVP. The real time change in the corrosion rate of carbon steel in acidic geothermal fluid in the presence of varying concentration of the polymeric inhibitor was observed. The decrease in the corrosion rate as immersion time is prolonged is due to the gradual formation of silica layer as promoted by the PVP formed on the metal surface. The effect of temperature on the corrosion rate of carbon steel in acidic geothermal fluid in the presence of varying concentration of the polymeric inhibitor was also considered to determine the applicability of PVP in actual geothermal systems. Evem at high temperature and pressured conditions, PVP was still able to inhibit the corrosion process. A possible mechanism of corrosion inhibition action of the polymeric inhibitor is proposed based on the results of the analysis made throughout the course of the study.

Successful fabrication of a polymer nanocomposite coating of PBZ modified with rubber with varying amounts of oMMT was made. The enhancement of the mechanical properties of PBZ-R by addition of MMT by its intercalation/exfoliation into the polymer matrix was supported by XRD, thermogravimetric tests, hardness test, and adhesion tests. Results of electrochemical measurements showed that the nanocomposite coatings exhibited good anti-corrosion property. PBZ-R alone offered corrosion protection to the carbon steel in acidic geothermal brine. This is due to the low water absorption capability of PBZ which prevents the corrosive fluid to penetrate into the coating. Addition of oMMT further increased the corrosion protection of the nanocomposite coating with an optimum loading of 5 % MMT. Addition of more than this amount would lead to agglomeration of nanofillers that would in turn negatively affect the mechanical properties of the nanocomposite as manifested by the hardness test. The stability and the protection efficiency was also evaluated under high temperature and high pressure. Based on the result, the PBZ-R-MMT nanocomposite was proven to be effective in protecting the steel even at

HT/HP conditions. This is due to the stability of the coating at the tested condition as supported by the thermal tests conducted.

## V. RECOMMENDATION

Despite the satisfactory results obtained from the studies conducted, it is still recommended to extend the study to dynamic conditions to simulate the actual line condition. Kinetics play a major role in various processes in the geothermal industry. It could have a significant effect on the inhibition and protection efficiencies of the tested polymeric materials.

A longer immersion time is also recommended to obtain a more accurate corrosion rates, especially in conducting weight loss analysis.

Comparative study of the performance of the nanocomposite synthesized with available coatings in the market is also recommended to further justify its application in acidic geothermal environment.

# VI. REFERENCES

1. Bertani, R. (2010). Geothermal Power Generation in the World 2005-2010 Update Report. *World Geothermal Congress 2010.* Bali, Indonesia.

2. Valdez, B., Schorr, M., Quintero, M., Carillo, M., Zlatev, R., Stoytcheva, M., et al. (2009). Corrosion and scaling at Cerro Prieto geothermal field. *Anti-corrosion Methods and Materials* , 28-34.

3. Casper, L.A. and Pinchback, T.R., (eds.), 1980, Geothermal scalingand corrosion: Philadelphia, American Society for Testing and Materials, 262 p. (ASTM, 1916 Race St., Philadelphia, PA 19103)

4. Jordan, O., Borromeo, C., Reyes, R., & Ferrolino, S. (2000). A Technical and Cost Assessment of Silica deposition in the Palinpinon-I geothermal field, Philippines, over 16 years of production and reinjection. *World Geothermal Congress.* Kyushu-Tohoku, Japan.

5. See, F. S. (2010). Silica Inhibitor Hot Injection Test at Bacman Geothermal Production Field, Botong, Philippines. *World Geothermal Congress.* Bali, Indonesia.

6. Horsup, D., Clark, J., Binks, B., Fletcher, P., & Hicks, J. (2007). I Put it in, But where does it go?"- The fate of corrosion inhibitors in multiphase systems. NACE Corrosion Conference and Expo. Houston, Texas: NACE

7. Panopio, A., Solis, R., & Fragata, J. (2008). F3680 Silica Inhibitor Testing in Botong Sector, Bacon-Manito Geothermal Production Field, Philippines. *GRC Transactions*, (pp. 231-236).

8. Mejorada, S., & Garcia, A. (2001). Geogard SX: A Silica Scale Inhibitor for Geothermal Brine. *Geothermal Resources Council Transactions* , 15-21.

9. Siega, F., Herras, E., & Buning, B. (2005). Calcite Scale Inhibition: The Case of Mahanagdong Wells in Leyte Geothermal Production Field, Philippines. *World Geothermal Congress.* Antalya, Turkey.

10. Remoroza, A., Doroodchi, E., & Moghtaderi, B. (2010). Corrosion Inhibition of Acid-Treated Geothermal Brine- results from Pilot Testing in Southern Negros, Philippines. *World Geothermal Congress 2010.* Bali, Indonesia.

11. Ramos-Candelaria, M. N. (2000). Calcite Inhibition Field Trials at MIndanao Geothermal Production Field (MGPF). *World Geothermal Congress.*

12. Arthur, D., Jonathan, A., Ameh, P., & Anya, C. (2013). A review on the assessment of polymeric materials used as corrosion inhibitor if metals and alloys. *International Journal of Industrial Chemistry* , 1-9.

13. Nogara, J., & Zarrouk, S. (2014). Evaluation of corrosion resistant alloys as construction material for acidic geothermal wells. *New Zealand Geothermal Workshop 2014 Proceedings*, (pp. 1-14). Auckland.

14. Amend, B., & Yee, J. (2013). Selective application of corrosion resistant alloys mitigates corrosion in pH-modified geothermal fluids. Corrosion Conference and Expo.

15. Wang, L., Wang, K., Chen, L., Zhang, Y.,He, C.(2006) Preparation,morphology and thermal/mechanical properties of epoxy/nanoclay composite. *Composites A,* 37:(11)1890–1896

16. Sancaktar,E. Kuznicki J.(2011) Nanocomposite adhesives: mechanical behavior with nanoclay.*International Journal of Adhesion and Adhesives*, 31:(5)286–300,

17. Keyoonwong,W., Kubouchi, M., Sakai,T., Aoki, S. (2009) Preparation of exfoliated epoxy/clay nanocomposite and its thermal & mechanical properties. *Proceedings of the International Symposium on Engineering, Energy and Environment (ISEEE09 '09)*, pp. 158–163, Rayong, Thailand.

18. Abacha, N., Sakai,T., Tsuda, K.,Kubouchi,M.(2007) Preparation and performance under corrosive environment of epoxynanocomposite. *Key Engineering Materials*, 353–358:(3)2167–2170

19. Yeh,J., Huang, H., Chen, C., Su, W.,Yu,Y. (2006) Siloxane-modified epoxy resin-clay nanocomposite coatings with advanced anticorrosive properties prepared by a solution dispersion approach. *Surface and Coatings Technology*, 200:( 8) 2753–2763, 2006.

20. de Leon, A., Pernites, R., & Advincula, R. (2012). Superhydrophobic Colloidally Textured Polythiophene Film as Superior Anticorrosion Coating. *Applied Materials and Interfaces* , 4: 3169−3176.

21. Gu, X., & Qiu, F. (2013). Synthesis and application of terpolymer scale inhibitor in the presence. Journal of Petroleum Science and Engineering , 109:177-186.

22. Guo, X., Qiu, F., Dong, K., Rong, X., He, K., Xu, J., et al. (2014). Preparation and application of copolymer modified with the palygorskite. *Applied Clay Science* , 99:187-193.

23. Guo, X., Qiu, F., Dong, K., XZhou, X., Qi, J., Zhou, Y., et al. (2012). Preparation, characterization and scale performance of scale inhibitor copolymer modification with chitosan. *Journal of Industrial and Engineering Chemistry* , 18:2177-2183.

24. Amjad, Z., & Koutsoukos, P. (2014). Evaluation of maleic acid based polymers as scale inhibitors. *Desalination* , 335:55-63.

25. Jensen, M., & Kelland, M. (2012). A new class of hyperbranched polymeric scale inhibitors. *Journal of Petroleum Science and Engineering* , 95: 66-72.

26. Spinthaki, A., Stathoulopoulou, A., & Demadis, K. (2015). The interplay between cationic polyethyleneimine and anionic polyelectrolytes for the control of silica scale formation in process waters. *International Journal of Corrosion and Scale Inhibition* , 2:125-138.

27. Gill, J. S. (2008). Scale Control in Geothermal Brines. *Transactions of Geothermal Resources Council 2008 Annual meeting.*

28. Gu, T., Liu, X., Chai, W., Li, B., & Sun, H. (2014). A preliminary research on polyvinyl alcohol hydrogel: A slowly-released anti-corrosion and scale inhibitor. *Journal of Petroleum Science and Engineering* , 122:453-457.

29. Mundhenk, H., Sanjua, B., Kohl, S., & Zorn, R. (2013). Corrosion and scaling as interrelated phenomena in an operating geothermal power plant. *Corrosion Science* , 17-28.

30. Iler, R. (1979). *The Chemistry of Silica; Solubility, Polymerization, Colloid and Surface Properties and Biochemistry of Silica.* John Wiley & Sons.

31. Kim, H., & Hwang, T. (2012). Corrosion protection enhancement effect by mixed silica nanoparticles of different sizes incorporated in a sol-gel silica film. . *J Sol-Gel Sci Technol* , 63:563-568.

32. Kumaraguru, S., Veeraraghavan, B., & Popov, B. (2006). Development of an Electroless Method to Deposit Corrosion-Resistant Silicate Layers on Metallic Substrates. *Journal of the Electrochemical Society* , 153:253-259.

33. Khelifa, F., Druart, M., Habibi, Y., Benard, F., Leclere, P., Olivier, M., et al. (2013). Sol-gel incorporation of silica nanofillers for tuning the anti-corrosion protection of acrylate-based coatings. *Progress in Organic Coatings* , 76: 900-911.

34. Emamgholizadeha, A., Rostamia, A., Omrania, A., & Rostamib, A. (2015). Performance of EP/PpPDA and EP/PpPDA/SiO2 nanocomposite on corrosion

inhibition of steel in hydrochloric acid solution. *Progress in organic Coatings* , 82: 7-16

35. Remoroza, A., Mejorada, A., & Salazar, A. (2008). Field Testing of pH Modification Silica Inhibition with Chemical Corrosion Inhibition. *Thiry-Third Workshop on Geothermal Reservoir Engineering.* Stanford, California.

36. Hermannsson, S. (1970). Corrosion of Metals and the Forming of a Protective Coating on the Inside of Pipes Carrying Thermal Waters Used by the Reykjavik Municipal Distrcit Heating Service. *Geothermics* , 2:1602-1612.

37. Lehrman, L., & Shuldener, H. (1952, August). Action of sodium silicate as a corrosion inhibitor in water piping. *Industrial and Engineering Chemistry* , 44(8):1765- 1769.

38. Arthur, D., Jonathan, A., Ameh, P., & Anya, C. (2013). A review on the assessment of polymeric materials used as corrosion inhibitor if metals and alloys. International Journal of Industrial Chemistry , 1-9.

39. Antonijevic, M., & Petrovi, M. (2008). Int.J.Electrochem.Sci , 1.

40. El-Maksuod, S. (2008). Int.J.Electrochem.Sci, 3 , 275.

41. Zheludkevich, Sachukin, & Yasakav. (2007). Anticorrosionn coatings with self-healing effect based on Nanocontainers impregnated with corrosion inhibitor. Chemistry of materials , 3: 402-411.

42. Thomas, G. (1981). Some new fundamental aspects in corrosion inhibition. 5th Euro. SYmp. Corr. Inhibitors, (p. 453). Ferrara, Italy.

43. Umoren, S., Ogbobe, O., Igwe, I., & Ebenso, E. (2008). Inhibition of Mild steel corrosion in acidic medium using synthetic and naturally occuring polymers and synergistic halide additives. Corr.Sci.,50(7) , 1998-2006.

44. Manimaran, N., Rajendran, S., Manivanan, M., & John Mary, S. (2012). Corrosion Inhibition of Carbon Steel By polyacrylamide. Res.J.Chem.Sci , 2(3), 52-57.

45. Finsgar, M., & Jackson, J. (2014). Application of corrosion inhibitors for steels in acidic media for the oil and gas industry: A review. Corr.Sci. , 86, 17-41.

46. Jing, C., & Hou, J. (2007). Sol-Gel derived Alumina/PVP hybrid nanocomposite film on metal for corrosion resistance. Journal of Apllied Polymer Science , 105: 697-705.

47. Graf, C., Vossen, D., Imhof, A., & van Blaaderen, A. (2003). A general method to coat colloidal particles with silica. Langmuir , 19: 6693-6700.

48. Lopez, A., Urena, A., & Rams, J. (2009). Surf Coat Technol , 203:1474-1480.

49. Pech, D., Steyer, P., & Millet, J. (2008). Corros Sci , 50:1492-1497.

50. Kim, H., & Hwang, T. (2012). Corrosion protection enhancement effect by mixed silica nanoparticles of different sizes incorporated in a sol-gel silica film. . J Sol-Gel Sci Technol , 63:563-568.

51. Daouadji, M. M., & Chelali, N. (2003). Influence of Molecular weight of Poly(otho-ethoxyaniline) on the corrosion inhibition efficiency of mild steel in acidic media. Journal of Applied Polymer Science , 91: 1275-1284.

52. Al Juhaiman, L., Mustafa, A., & Mekhamer, W. (2012). Int.J.Electrochem.Sci.,7 , 8578-8596.

53. Salehi, M., Nasr-Esfahani, M., Sharifian-Esfahani, A., & Ekramian, E. (2011). Magnetite/Polyvinylpyrrolidone Nanocomposite: Green Simple Fabrication and Characterization. 2nd International Conference on Chemistry and Chemical Engineering (pp. 174-177). Singapore: IACSIT Press.

54. Hermannsson, S. (1970). Corrosion of Metals and the Forming of a Protective Coating on the Inside of Pipes Carrying Thermal Waters Used by the Reykjavik Municipal Distrcit Heating Service. Geothermics , 2:1602-1612.

55. Iler, R. (1979). The Chemistry of Silica; Solubility, Polymerization, Colloid and Surface Properties and Biochemistry of Silica. John Wiley & Sons.

56. Remoroza, A., Mejorada, A., & Salazar, A. (2008). Field Testing of pH Modification Silica Inhibition with Chemical Corrosion Inhibition. Thiry-Third Workshop on Geothermal Reservoir Engineering. Stanford, California.

57. Demadis, K., & Neofotistiu, E. (2004). Inhibition and Growth Control of Colloidal Silica: Designed Chemical Approaches. Materials Performance , 38-41.

58. Sanchez, D., Herras, E., Siega, F., S. N., Nogara, J., & Sambrano, B. *Evaluation of NaOH Injection into Acid Wells of Leyte Geothermal Production Field and MIndanao 1 Geothermal Project: The Case of MG9D and KN2D Wells.* Makati: EDC.

59. Vallejos-Ruiz, O., S.-R. E., & Gonzalez-Vargas, C. (2005). Reservoir Management in the Miravalles Geothermal Field, Costa Rica. *Proceedings Geothermal World Congress* (pp. 1-8). Antalya: International Geothermal Association.

60. Ishida, H., Agag, T., Eds. *Handbook of Benzoxazine Resins;* Elsevier, 2011

61. Zhou, C., Lu, X., Xin, Z., & Liu, J. (2013). Corrosion resistance of novel silane-functional polybenzoxazine coating on steel. *Corrosion Science , 70*, 145-151.

62. Ishida, H.; Allen, D. J.. *J. Polym. Sci, Part B: Polym. Phys.***1996,***34,* 1019-1030.

63. Jang, J., & Yang, H. (2000). Toughness improvement of carbon-fibre/polybenzoxazine composites by rubber modification. *Composites Science and Technology , 60* (3), 457-463.

64. Hung, W.,Chang,K., Chang,,Y.,Yeh,J. (2011). Advanced anticorrosive coatings prepared from polymer-clay nanocomposite materials, in: B. Reddy (Ed.), Advances in Nanocomposites—Synthesis, Characterization and Industrial Applications, InTech, ISBN: 978-953-307-165-7

65. Lan, T.; Kaviratna, P. D. & Pinnavaia, T. (1994). On the Nature of Polyimide-Clay Hybrid Composites. J. Chem. Mater.. 6, 573-575.

66. Tyan, H. -L.; Liu, Y. -C. & Wei, K. -H. (1999). Thermally and Mechanically Enhanced Clay/Polyimide Nanocomposite via Reactive Organoclay. Chem. Mater. 11, 1942- 1947.

67.Wang, K. H.; Choi, M. H.; Koo, C. M.; Choi, Y. S. & Chung, I. J. (2001). Synthesis and characterization of maleated polyethylene/clay nanocomposites. Polymer, 42, 9819-9826.

68. Azeez,A., Rhee,K., Park, S., Hui,D.(2012). Epoxy clay nanocomposites- processing, properties and applications: A review. *Composites Part B*

69. Manias, E, A Touny, L Wu, K Strawhecker, B Lu, and C Chung. *Chem.Mater.*, 2001: 13:3516-3523.

70. Alexander, M., & Dubois, P. (2000). Polymer-layered silicate nanocomposites: preparation, properties, and uses of a new class of materials. *Materials Science Engineering , 28*, 1-63.

71. Karickhoff, S., & Bailey, G. (1973). *Clays and Clay Minerals* , 21:59-70.

72. Corcione, C., & Frigione, M. (2012). *Materials* , 5:2960-2980.

73. Yang, K. K.; Wang, X. L. & Wang, Y. Z. (2007). Progress in nanocomposite of biodegradable polymer. J. Ind. Eng. Chem. 13, 485-500.
BIBLIOGRAPHY \l 1033 Allen, D., & Ishida, H. (2009). Effect of phenol substitution on the network structure and properties of linear aliphatic diamine-based benzoxazines. *Polymer , 50* (2), 613-626.

74. Allen, D., & Ishida, H. (2006). Physical and Mechanical Properties of Flexible Polybenzoxazine Resins: Effect of Aliphatic Diamine Chain Length. *Journal of Applied Polymer Science , 101*, 2798-2809.

75. Antonijevic, M., & Petrovi, M. (2008). *Int.J.Electrochem.Sci* , 1.

76. Jang, J., & Yang, H. (2000). Toughness improvement of carbon-fibre/polybenzoxazine composites by rubber modification. *Composites Science and Technology , 60* (3), 457-463.

77. Lee, Y., Allen, D., & Ishida, H. (2006). Effect of Rubber Reactivity on the Morphology of Polybenzoxazine Blends Investigated by Atomic Force Microscopy and Dynamic Mechanical Analysis. *Journal of Applied Polymer Science , 100*, 2443-2454.

78. Liu, H., Su, W., & Liu, Y. (2011). Self-assembled benzoxazine-bridged polysilsesquioxanes exhibiting ultralow-dielectric constants and yellow-light photoluminescent emission. *J. Mater. Chem. , 21*, 7182-7187.

79. Lopez, A., Urena, A., & Rams, J. (2009). *Surf Coat Technol* , 203:1474-1480.

80. Malik, M., Ali Hashim, M., Nabi, F., & AL-Thabait, S. (2011). *Int.J.Electrochem.Sci., 6* , 1927-1948.

81. Sperling, L. H. (2006). *Introduction to physical polymer science* (Fourth ed.). John Wiley & Sons, Inc.

82. Strehblow, H., & Marcus, P. (2012). Fundamentals of corrosion. In P. Marcus, *Corrosion mechanisms in theory and practice.* Taylor and Francis Group.

83. Swift, G., Carraher, C., & Bowman, C. (1997). *Polymer modification.* Springer.

84. Takeichi, T., Kano, T., & Agag, T. (2005). Synthesis and thermal cure of high molecular weight polybenzoxazine precursors and the properties of the thermosets. *Polymer , 46*, 12172-12180.

85. Wang, C., Su, Y., Kuo, S., Huang, C., Sheen, Y., & Chang, F. (2006). Low-surface-free-energy materials based on polybenzoxazines. *Angew. Chem. Int. Ed. , 45*, 2248-2251